

Fermion masses and flavor mixings and strong CP problem

Y. H. Ahn

*Key Laboratory of Particle Astrophysics, Institute of High Energy Physics,
Chinese Academy of Sciences, Beijing, 100049, China**

Abstract

For all the success of the Standard Model (SM), it is on the verge of being surpassed. In this regard we argue, by showing a minimal flavor-structured model based on the non-Abelian discrete $SL_2(F_3)$ symmetry, that $U(1)$ mixed-gravitational anomaly cancellation could be of central importance in constraining the fermion contents of a new chiral gauge theory. Such anomaly-free condition together with the SM flavor structure demands a condition $k_1 X_1/2 = k_2 X_2$ with X_i being a charge of $U(1)_{X_i}$ and k_i being an integer, both of which are flavor dependent. We show that axionic domain-wall condition N_{DW} with the anomaly free-condition depends on both $U(1)_X$ charged quark and lepton flavors; the seesaw scale congruent to the scale of Peccei-Quinn symmetry breakdown can be constrained through constraints coming from astrophysics and particle physics. Then the model extended by $SL_2(F_3) \times U(1)_X$ symmetry can well be flavor-structured in a unique way that $N_{\text{DW}} = 1$ with the $U(1)_X$ mixed-gravitational anomaly-free condition demands additional Majorana fermion and the flavor puzzles of SM are well delineated by new expansion parameters expressed in terms of $U(1)_X$ charges and $U(1)_X$ - $[SU(3)_C]^2$ anomaly coefficients. And the model provides remarkable results on neutrino (hierarchical mass spectra and unmeasurable neutrinoless-double-beta decay rate together with the predictions on atmospheric mixing angle and leptonic Dirac CP phase favored by the recent long-baseline neutrino experiments), QCD axion, and flavored-axion.

*Electronic address: axionahn@naver.com

I. INTRODUCTION

Symmetries play an important role in physics in general and in quantum field theory in particular. The standard model (SM) as a low-energy effective theory has been very predictive and well tested, due to the symmetries satisfied by the theory - Lorentz invariance plus the $SU(3)_C \times SU(2)_L \times U(1)_Y$ gauge symmetry in addition to the discrete space-time symmetries like P and CP. However, it leaves many open questions for theoretical and cosmological issues that have not been solved yet. These include the following: inclusion of gravity in gauge theory, instability of the Higgs potential, cosmological puzzles of matter-antimatter asymmetry, dark matter, dark energy, and inflation, and flavor puzzle associated with the SM fermion mass hierarchies, their mixing patterns with the CP violating phases, and the strong CP problem. Moreover, there is no answer to the question: why there are three generations in the SM. The SM, therefore, cannot be the final answer. So it is widely believed that the SM should be extended a more fundamental underlying theory. Neutrino mass and mixing is the first new physics beyond SM and adds impetus to solving the open questions in particle physics and cosmology. Moreover, a solution to the strong CP problem of QCD through Peccei-Quinn (PQ) [1] mechanism¹ may hint a new extension of gauge theory realized in gauge/gravity duality [2]. If nature is stringy, string theory, the only framework we have for a consistent theory with both quantum mechanics and gravity, should give insight into all such fundamental issues. String theory when compactified to four dimensions can generically contain $G_F = \textit{anomalous gauged } U(1) \textit{ plus non-Abelian finite symmetries}$. In this regard, in order to construct a model with the open questions one needs more types of gauge symmetry beside the SM gauge theory. One of simple approaches to a neat solution for those could be accommodated by a type of symmetry based on seesaw [4] and Froggatt-Nielsen (FN) [5] frameworks, since it is widely believed that non-renormalizable operators in the effective theory should come from a more fundamental underlying renormalizable theory by integrating out the heavy degrees of freedom. Therefore, one can anticipate that there may exist some correlations between low energy and high energy physics; *e.g.* the flavored-axion [2] can easily fit into a string theoretic framework, and appear cosmologically as a form of cold dark matter. Even gravity (which is well-

¹ See, its related reports [3].

described by Einstein’s general theory of relativity) lies outside the purview of the SM, once the gauged $U(1)$ s are introduced in an extended theory, its mixed gravitational-anomaly should be free. And we assume that the heavy gauge bosons associated with the gauged $U(1)$ s are decoupled, and thus in the model we consider the gauged $U(1)$ s will be treated as the global $U(1)$ s symmetries at low energy. As shown in Ref.[2], the FN mechanism formulated with global $U(1)$ flavor symmetry could be promoted from the string-inspired gauged $U(1)$ symmetry. Such flavored-PQ global symmetry $U(1)$ acts as a bridge for the flavor physics and string theory [2, 6]. Flavor modeling on the non-Abelian finite group has been recently singled out as a good candidate to depict the flavor mixing patterns, *e.g.*, Ref. [2, 7, 8], since it is preferred by vacuum configuration for flavor structure. Hence, flavored-PQ symmetry modeling extended to G_F could be a powerful tool to resolve the open questions for particle physics and cosmology.

In this paper we present, by showing an extended flavored-PQ model which extend to a compact symmetry² G_F for new physics beyond SM, that the $U(1)$ mixed-gravitational anomaly cancellation is of central importance in constraining the fermion contents of a new chiral gauge theory, and the flavor structure of G_F is³ strongly correlated with physical observables. So, finding the SM fermion mass spectra and their peculiar flavor mixing patterns in modeling is very important, since it is the first step toward establishing an effective low-energy Lagrangian of an extended theory. Unlike the A_4 symmetry containing one- and three-dimensional representations used in Refs.[2, 8] the non-abelian discrete $SL_2(F_3)$ symmetry [7, 9, 10] contains two-dimensional representation in addition to one- and three-dimensional representations, in which the three dimensional representation is mainly responsible for the large leptonic mixing angles while the two dimensional representation is mainly to fit the quark masses and small mixing angles (especially the Cabbibo angle). Moreover, depending on the quantum number of flavored $U(1)_X$ the group G_F can give different structures of quark and lepton mass texture. Together with $U(1)_X$ symmetry, such $SL_2(F_3)$ could make the model compact providing an economic mass texture (see Eq. (21))

² Here the meaning of a ‘compact’ symmetry is a symmetry that provides only requisite parameters it is not hard to disprove; for example, see the quark and lepton mass textures in Eqs. (21) and (64) provided by the well-sewed supepotentials (18) and (45) under the $SL_2(F_3) \times U(1)_X$ symmetry.

³ Here we assume that, below the scale associated with $U(1)_{X_i}$ gauge bosons, the gauged $U(1)_{X_i}$ leaves behind low-energy symmetries which are QCD anomalous global $U(1)_{X_i}$, see Eq. (1).

for the quark mass spectra and mixings, especially, the Cabbibo angle. On the other hand, if one uses A_4 symmetry in the same framework, it is expected that there are uncontrollable redundant parameters in the quark mass textures which should be fine-tuned by hand to realize the quark mass spectra and mixings. So taking $G_F = SL_2(F_3) \times U(1)_X$ may have a good advantage to compactly describe the peculiar mixing patterns of quarks and leptons including their masses. Contrary to Ref. [11], the present model provides another possibility of flavor modeling in virtue of the quantum number of $U(1)_X$, leading to completely different mass textures of quark and lepton. And in turn its results give an upper bound on QCD axion mass with different values of $\tan \beta$ in Eq. (32) and g_{Aee} in Eq. (58), since axion to leptons and quarks couplings depend on structure of the quark and lepton sector. In this sense, if the astronomical constraint of star cooling [12] favored by the model in Ref. [11] is really responsible for the QCD axion, the present model will be ruled out. And it is expected that the upcoming NA62 experiment expected to reach the sensitivity of $\text{Br}(K^+ \rightarrow \pi^+ + A_i) < 1.0 \times 10^{-12}$ [13] will soon rule out or favor the scenario in Ref. [11], while for the present model just gives an upper bound on the scale of PQ symmetry breakdown.

The rest of this paper is organized as follows. In Sec. II we set up a minimalistic SUSY model for quarks, leptons, and flavored-axions (and its combination QCD axion), which contains a $G_F = SL_2(F_3) \times U(1)_X$ symmetry for a compact description of new physics beyond SM. In Sec. III the $SL_2(F_3) \times U(1)_X$ symmetry-invariant superpotential for vacuum configurations is constructed and its vacuum structure is analyzed. In Sec. IV we describe the Yukawa superpotential for quarks and flavored-axions and show that the SM quark masses and mixings could well be described by new expansion parameters defined under the $U(1)_X \times [\text{gravity}]^2$ anomaly-free condition. In turn, in order to show that the quark sector works well we perform a numerical simulation. And we show that the constraint coming from the particle physics on rare decay $K^+ \rightarrow \pi^+ + A_i$ [11, 14, 15] on the $U(1)_X$ symmetry breaking scale is much stronger than that from the astroparticle physics on QCD axion cooling of stars. Along the line of quark sector, in Sec. V we show that the Yukawa superpotential for leptons and flavored-axions could well be flavor-structured, which gives testable predictions on the neutrino mass ordering, δ_{CP} and θ_{23} . And we show that the $U(1)_X$ symmetry breaking scale can also be constrained via the astrophysical constraint on flavored-axion cooling of stars, but its constraint is smaller than that from $K^+ \rightarrow \pi^+ + A_i$. What we have done is summarized in Sec. VI, and we provide our conclusions. In appendix

we consider possible next-to-leading order corrections.

II. THE MODEL SETUP

Assume we have a SM gauge theory based on the $G_{\text{SM}} = SU(3)_C \times SU(2)_L \times U(1)_Y$ gauge group, and that the theory has in addition a $G_F = SL_2(F_3) \times U(1)_X$ for a *compact* description of new physics beyond SM. Here the symmetry group of the double tetrahedron $SL_2(F_3)$ [7, 9, 10]⁴ is mainly for the peculiar flavor mixing patterns. Here we assume that the non-Abelian finite group $SL_2(F_3)$ could be realized in field theories on orbifolds and it is a subgroup of a gauge symmetry that can be protected from quantum-gravitational effects. Since chiral fermions are certainly a main ingredient of the SM, the gauge- and gravitational-anomalies of the gauged $U(1)_X$ are⁵ generically present, making the theory inconsistent, where

$$U(1)_X \equiv U(1)_{X_1} \times U(1)_{X_2}. \quad (1)$$

Some requirements and constraints needed for the extended theory are:

- (i) The mixed $G_{\text{SM}} \times U(1)_{X_i} \times U(1)_{X_j}$ and cubic $U(1)_{X_i} \times [U(1)_{X_j}]^2$ anomalies should be cancelled by the Green-Schwarz (GS) mechanism [18]. Hereafter the gauged $U(1)$ will be treated as the global $U(1)$ symmetry. Note that the global symmetry $U(1)_X$ we consider is the remnant of the $U(1)_X$ gauge symmetry broken by the GS mechanism. Hence, the spontaneous breaking of $U(1)_X$ realizes the existence of the Nambu-Goldstone (NG) modes (called axions) and provides an elegant solution to the strong CP problem.
- (ii) The non-vanishing anomaly coefficient of the quark sector $\{U(1)_{X_i} \times [\textit{gravity}]^2\}_{\text{quark}}$ constrains the quantity $\sum_j^{N_f} X_{\psi_j}$ in the gravitational instanton backgrounds (with N_f generations well defined in the non-Abelian discrete group), and in turn whose

⁴ The details of the $SL_2(F_3)$ group are shown in Appendix A.

⁵ As shown in Refs. [2, 6] with the well-defined Kahler potential based on type-IIB string theory, the author demonstrated that, while the two massive gauge bosons associated with the gauged $U(1)_{X_i}$ eat two degree of freedom, the other two axionic directions survive to low energies as the flavored-PQ axions, leaving behind low energy symmetries which are the QCD anomalous global $U(1)_{X_i}$.

quantity is congruent to the $U(1)_{X_i} \times [SU(3)_C]^2$ anomaly coefficient

$$\delta_k^G \delta^{ab} = 2 \sum_{\psi_i} X_{k\psi_i} \text{Tr}(t^a t^b), \quad (2)$$

in the QCD instanton backgrounds, where the t^a are the generators of the representation of $SU(3)$ to which Dirac fermion ψ_i belongs with X -charge. Thanks to the two QCD anomalous $U(1)$ we have a relation [8]

$$|\delta_1^G / \delta_2^G| = |f_{a_1} / f_{a_2}|, \quad (3)$$

indicating that the ratio of QCD anomaly coefficients is fixed by that of the decay constants f_{a_i} of the flavored-axions A_i . Here f_{a_i} set the flavor symmetry breaking scales, and their ratios appear in expansion parameters of the quark and lepton mass spectra (see Eqs. (24) and (25)). As studied in Refs. [2, 8], in the so-called flavored-PQ models the scale of PQ symmetry breakdown is congruent to the seesaw scale via Eq. (3), which could well be fixed⁶ and/or constrained through the constraints and/or hints coming from astroparticle physics on axion cooling of stars with the fine-structure of axion to electron $\alpha_{Aee} < 6 \times 10^{-27}$ [17], $4.1 \times 10^{-28} \lesssim \alpha_{Aee} \lesssim 3.7 \times 10^{-27}$ [17], and the coupling of axion to neutron $g_{Ann} < 8 \times 10^{-10}$ [21] etc. as well as the constraints coming from particle physics on rare flavor violating decay processes induced by the flavored-axions $\text{Br}(K^+ \rightarrow \pi^+ A_i) < 7.3 \times 10^{-11}$ [16] and $\text{Br}(\mu \rightarrow e \gamma A_i) \lesssim 1.1 \times 10^{-9}$ [22] etc..

- (iii) The mixed-gravitational anomaly $U(1)_X \times [gravity]^2$ must be cancelled to consistently couple gravity to matter charged under $U(1)_X$. Since a heavy Majorana neutrino (necessary to implement the seesaw and PQ mechanisms, simultaneously) with $U(1)_{X_1}$ charge $X_1/2$ does not have a vanishing $U(1)_{X_1} \times [gravity]^2$ anomaly, its anomaly should be cancelled by another contribution of $U(1)_{X_2} \times [gravity]^2$ anomaly. Hence, the $U(1)_X$ charges of SM fermions and new fermions including heavy Majorana neutrinos must be commensurate through the $U(1)_X \times [gravity]^2$ anomaly satisfying a condition

$$k_1 X_1/2 = k_2 X_2 \quad (4)$$

⁶ If one takes seriously the hints from axion cooling of stars in Refs. [17, 20], one can fix the scale of PQ symmetry breakdown congruent to the seesaw scale [2].

where ⁷ k_i ($i = 1, 2$) are nonzero integers, which is a conjectured relationship between two anomalous $U(1)$ s. The $U(1)_{X_i}$ is broken down to its discrete subgroup Z_{N_i} in the backgrounds of QCD instanton, and the quantities N_i (*nonzero integers*) associated to the axionic domain-wall are given by

$$\left| \frac{\delta_1^G}{X_1/2k_2} \right| = N_1, \quad \left| \frac{\delta_2^G}{X_2/k_1} \right| = N_2. \quad (5)$$

Then, from Eqs. (4) and (5) one obtains $|\delta_1^G| = N_1$ and $|\delta_2^G| = N_2$. Clearly, in the QCD instanton backgrounds if N_1 and N_2 are relative prime, there is no $Z_{N_{\text{DW}}}$ discrete symmetry and therefore no domain wall problem⁸. Now, we will see that the domain-wall condition with the $U(1)_X \times [\text{gravity}]^2$ anomaly free-condition is dependent on the $U(1)_X$ charged quark and lepton flavors. Eq. (2) can be expressed $\delta_1^G = \alpha X_1$ and $\delta_2^G = \omega X_2$, where α and ω are some integer numbers. To make sure that no axionic domain-wall problem occurs, the following two conditions are required: (i) *The numbers α and ω coming from $U(1)_X$ charged quark flavors should be ‘relative prime’*. If the quantum numbers X_1 and X_2 are given by $-2p$ and $-q$, respectively, from Eq. (4) one obtains $k_1 p = k_2 q$. So the number k_i coming from the $U(1)_X \times [\text{gravity}]^2$ anomaly-free condition depends on both the $U(1)_X$ charged quark and lepton flavors. Then, Eq. (5) is expressed as

$$N_1 = |\delta_1^G| = 2|\alpha| k_2, \quad N_2 = |\delta_2^G| = |\omega| k_1. \quad (6)$$

(ii) Hence, *the number k_2 should be relative prime with $|\omega|$ and k_1 , as well as the number k_1 should not be a multiple of 2 and should be relative prime with $|\alpha|$.*

Consequently⁹, under the $U(1)_X \times [\text{gravity}]^2$ anomaly-free condition, to make sure that no axionic domain-wall problem occurs in a theory one could introduce additional $U(1)_X$ charged Majorana fermions and/or could assign well flavor-structured $U(1)_X$ quantum numbers to fermion contents that can protect k_1 to be a multiple of 2.

⁷ For $-k_1 = k_2 = 1$ in Ref. [2], additional Majorana fermions are introduced to satisfy the $U(1)_X \times [\text{gravity}]^2$ anomaly free-condition. Note that, however, in general, $k_2/k_1 \neq \text{integer}$.

⁸ Note that, in the present model, since the non-Abelian finite symmetry $SL_2(F_3)$ is broken completely by higher order effects, there is no residual symmetry; so, there is no room for a spontaneously broken discrete symmetry to lead to domain-wall problem.

⁹ Of course, one can consider the cases of the domain-wall number $N_{\text{DW}} > 1$ if the PQ phase transition occurred during (or before) inflation.

As we shall see later, even though the integer k_i depends on both the $U(1)_X$ charged quark and lepton flavors, it does not play the role of constraining the QCD axion decay constant $F_A = f_{a_i}/\delta_i^G\sqrt{2}$ through physical processes induced by flavored-axions in the flavored-PQ models. On the other hand, those physical processes are constrained by 2α and ω coming from the QCD instanton background.

Along this line, the G_F quantum number of the field contents is assigned in the following two ways: (a) in a way that the $SL_2(F_3)$ that compactly depict the Cabbibo-Kobayashi-Maskawa (CKM) for quark mixings and Pontecorvo-Maki-Nakagawa-Sakata (PMNS) for leptonic mixings requires a desired vacuum configuration, and (b) the $U(1)_X$ mixed-gravitational anomaly-free condition with the SM flavor structure demands additional Majorana fermions as well as no axionic domain-wall problem.

III. VACUUM CONFIGURATION

In this section, the $SL_2(F_3) \times U(1)_X$ symmetry-invariant superpotential for vacuum configurations is constructed and its vacuum structure is analyzed. First we present the representations of the field contents responsible for vacuum configuration. Apart from the usual two Higgs doublets $H_{u,d}$ responsible for electroweak symmetry breaking, which are invariant under $SL_2(F_3)$ (*i.e.* flavor singlets **1**), the scalar sector is extended via two types of new scalar multiplets, flavon fields responsible for the spontaneous breaking of the flavor symmetry $\Phi_T, \Phi_S, \Theta, \tilde{\Theta}, \eta, \Psi, \tilde{\Psi}$ that are G_{SM} -singlets and driving fields $\Phi_0^T, \Phi_0^S, \eta_0, \Theta_0, \Psi_0$ that are to break the flavor group along required vacuum expectation value (VEV) directions and to allow the flavons to get VEVs, which couple only to the flavons: we take the flavon fields Φ_T, Φ_S to be $SL_2(F_3)$ triplets, η to be a $SL_2(F_3)$ doublet (**2'** representation), and $\Theta, \tilde{\Theta}, \Psi, \tilde{\Psi}$ to be $SL_2(F_3)$ singlets (**1** representation), respectively, that are G_{SM} -singlets, and driving fields Φ_0^T, Φ_0^S to be $SL_2(F_3)$ triplets, η_0 to be a $SL_2(F_3)$ doublet (**2''** representation) and Θ_0, Ψ_0 to be $SL_2(F_3)$ singlets. The flavored-PQ symmetry $U(1)_X$ is composed of two anomalous symmetries $U(1)_{X_1} \times U(1)_{X_2}$ generated by the charges $X_1 \equiv -2p$ and $X_2 \equiv -q$. The flavon fields $\{\Phi_S, \Theta, \tilde{\Theta}\}$ are X_1 charged, and $\{\Phi_0^S, \Theta_0\}$ are $-2X_1$ charged, respectively, under $U(1)_{X_1}$; the field Ψ ($\tilde{\Psi}$) is X_2 ($-X_2$) charged under $U(1)_{X_2}$. For vacuum stability and a desired vacuum alignment solution, we enforce $\{\Phi_T, \eta\}$ to be neutral under $U(1)_X$. And the others $H_{u,d}, \Phi_0^T, \eta_0$, and Ψ_0 are neutral under $U(1)_X$. Moreover, the superpotential W in the

theory is uniquely determined by the $U(1)_R$ symmetry, containing the usual R -parity as a subgroup: $\{matter\ fields \rightarrow e^{i\xi/2} matter\ fields\}$ and $\{driving\ fields \rightarrow e^{i\xi} driving\ fields\}$, with $W \rightarrow e^{i\xi} W$, whereas flavon and Higgs fields remain invariant under an $U(1)_R$ symmetry. As a consequence of the R symmetry, the other superpotential term $\kappa_\alpha L_\alpha H_u$ and the terms violating the lepton and baryon number symmetries are not allowed. In addition, dimension 6 supersymmetric operators like $Q_i Q_j Q_k L_l$ (i, j, k must not all be the same) are not allowed either, and stabilizing proton. Here the global $U(1)$ symmetry is a remnant of the broken $U(1)$ gauge symmetry which can connect string theory with flavor physics [2, 6] (see also [23]).

Under $SL_2(F_3) \times U(1)_X \times U(1)_R$, representations of the driving, flavon, and Higgs fields are summarized as in Table I. The superpotential depending on the driving fields, invariant

TABLE I: Representations of the driving, flavon, and Higgs fields under $SL_2(F_3) \times U(1)_X \times U(1)_R$. Here $U(1)_X \equiv U(1)_{X_1} \times U(1)_{X_2}$ symmetries which are generated by the charges $X_1 = -2p$ and $X_2 = -q$.

Field	Φ_0^T	Φ_0^S	Θ_0	Ψ_0	η_0	Φ_S	Φ_T	Θ	$\tilde{\Theta}$	Ψ	$\tilde{\Psi}$	η	H_d	H_u
$SL_2(F_3)$	3	3	1	1	2''	3	3	1	1	1	1	2'	1	1
$U(1)_X$	0	$4p$	$4p$	0	0	$-2p$	0	$-2p$	$-2p$	$-q$	q	0	0	0
$U(1)_R$	2	2	2	2	2	0	0	0	0	0	0	0	0	0

under $G_{SM} \times U(1)_R \times G_F$, reads at leading order

$$\begin{aligned}
W_v = & \Phi_0^T(\mu_T \Phi_T + g_T \Phi_T \Phi_T) + \Phi_0^S(g_1 \Phi_S \Phi_S + g_2 \tilde{\Theta} \Phi_S) + \eta_0(\mu_\eta \eta + g_\eta \eta \Phi_T) \\
& + \Theta_0(g_3 \Phi_S \Phi_S + g_4 \Theta \Theta + g_5 \Theta \tilde{\Theta} + g_6 \tilde{\Theta} \tilde{\Theta}) + g_7 \Psi_0(\Psi \tilde{\Psi} - \mu_\Psi^2) + g_8 \Phi_0^T \eta \eta, \quad (7)
\end{aligned}$$

where higher dimensional operators are neglected, and $\mu_{i=T,\Psi,\eta}$ are dimensional parameters and $g_{T,\eta}, g_{1,\dots,8}$ are dimensionless coupling constants. Note here that the model implicitly has two $U(1)_X \equiv U(1)_{X_1} \times U(1)_{X_2}$ symmetries which are generated by the charges $X_1 = -2p$ and $X_2 = -q$. The fields Ψ and $\tilde{\Psi}$ charged by $-q, q$, respectively, are ensured by the $U(1)_X$ symmetry extended to a complex $U(1)$ due to the holomorphy of the superpotential. So, the PQ scale $\mu_\Psi = \sqrt{v_\Psi v_{\tilde{\Psi}}/2}$ corresponds to the scale of spontaneous symmetry breaking of the $U(1)_{X_2}$ symmetry. Since there is no fundamental distinction between the singlets Θ and $\tilde{\Theta}$ as indicated in Table I, we are free to define $\tilde{\Theta}$ as the combination that couples to $\Phi_0^S \Phi_S$ in

the superpotential W_v [24]. At the leading order the usual superpotential term $\mu H_u H_d$ is not allowed, while at the leading order the operator driven by Ψ_0 and at the next leading order the operators driven by Φ_0^T and η_0 are allowed

$$g_{\Psi_0} \Psi_0 H_u H_d + \frac{g_{T_0}}{\Lambda} (\Phi_0^T \Phi_T)_1 H_u H_d + \frac{g_{\eta_0}}{\Lambda} (\eta_0 \eta)_1 H_u H_d, \quad (8)$$

which is to promote the effective μ -term $\mu_{\text{eff}} \equiv g_{\Psi_0} \langle \Psi_0 \rangle + g_{T_0} \langle \Phi_0^T \rangle v_T / (\sqrt{2} \Lambda) + g_{\eta_0} \langle \eta_0 \rangle v_\eta / (\sqrt{2} \Lambda)$ of the order of m_S , $m_S v_T / \Lambda$, and $m_S v_\eta / \Lambda$ (here $\langle \Psi_0 \rangle$, $\langle \Phi_0^T \rangle$, and $\langle \eta_0 \rangle$: the VEVs of the scalar components of the driving fields, m_S : soft SUSY breaking mass). It is interesting that at the leading order the electroweak scale does not mix with the potentially large scales, the VEVs of the scalar components of the flavon fields, $v_S, v_T, v_\Theta, v_\eta$ and v_Ψ . Actually, in the model once the scale of breakdown of $U(1)_X$ symmetry is fixed by the constraints coming from astrophysics and particle physics, the other scales are automatically fixed by the flavored model structure. And it is clear that at the leading order the scalar supersymmetric $W(\Phi_T \Phi_S)$ terms are absent due to different $U(1)_X$ quantum numbers, which is crucial for relevant vacuum configuration in the model to produce compactly the present lepton and quark mixing angles. Now we consider how a desired vacuum configuration for compact description of quark and lepton mixings could be derived. In SUSY limit, the vacuum configuration is obtained by the F -terms of all fields being required to vanish. The vacuum alignments of the flavons Φ_T and η are determined by

$$\begin{aligned} \frac{\partial W_v}{\partial \Phi_{01}^T} &= \mu_T \Phi_{T1} + \frac{2g_T}{3} (\Phi_{T1}^2 - \Phi_{T2} \Phi_{T3}) + i g_8 \eta_1^2 = 0, \\ \frac{\partial W_v}{\partial \Phi_{02}^T} &= \mu_T \Phi_{T3} + \frac{2g_T}{3} (\Phi_{T2}^2 - \Phi_{T1} \Phi_{T3}) + g_8 (1 - i) \eta_1 \eta_2 = 0, \\ \frac{\partial W_v}{\partial \Phi_{03}^T} &= \mu_T \Phi_{T2} + \frac{2g_T}{3} (\Phi_{T3}^2 - \Phi_{T1} \Phi_{T2}) + g_8 \eta_2^2 = 0 \end{aligned} \quad (9)$$

$$\begin{aligned} \frac{\partial W_v}{\partial \eta_{01}} &= \mu_\eta \eta_2 + \frac{5g_\eta}{6} \left(\frac{1-i}{2} \eta_2 \Phi_{T1} + i \eta_1 \Phi_{T3} \right) = 0 \\ \frac{\partial W_v}{\partial \eta_{02}} &= -\mu_\eta \eta_1 + \frac{5g_\eta}{6} \left(\frac{1-i}{2} \eta_1 \Phi_{T1} + i \eta_2 \Phi_{T2} \right) = 0 \end{aligned} \quad (10)$$

From this set of five equations, we can obtain the supersymmetric vacua for Φ_T and η

$$\begin{aligned} \langle \Phi_T \rangle &= \left(\frac{v_T}{\sqrt{2}}, 0, 0 \right), \quad \text{with } \mu_T = -g_T \frac{\sqrt{2}}{3} v_T - i \frac{g_8}{\sqrt{2}} \frac{v_\eta^2}{v_T}, \\ \langle \eta \rangle &= \left(\pm \frac{v_\eta}{\sqrt{2}}, 0 \right), \quad \text{with } \mu_\eta = g_\eta \frac{v_T}{\sqrt{2}} \frac{5(1-i)}{12}, \end{aligned} \quad (11)$$

where g_T and g_η are dimensionless couplings, and v_T and v_η are not determined. The minimization equations for the vacuum configuration of Φ_S and $(\Theta, \tilde{\Theta})$ are given by

$$\begin{aligned}\frac{\partial W_v}{\partial \Phi_{01}^S} &= \frac{2g_1}{3} (\Phi_{S1}\Phi_{S1} - \Phi_{S2}\Phi_{S3}) + g_2\Phi_{S1}\tilde{\Theta} = 0, \\ \frac{\partial W_v}{\partial \Phi_{02}^S} &= \frac{2g_1}{3} (\Phi_{S2}\Phi_{S2} - \Phi_{S1}\Phi_{S3}) + g_2\Phi_{S3}\tilde{\Theta} = 0, \\ \frac{\partial W_v}{\partial \Phi_{03}^S} &= \frac{2g_1}{3} (\Phi_{S3}\Phi_{S3} - \Phi_{S1}\Phi_{S2}) + g_2\Phi_{S2}\tilde{\Theta} = 0, \\ \frac{\partial W_v}{\partial \Theta_0} &= g_3 (\Phi_{S1}\Phi_{S1} + 2\Phi_{S2}\Phi_{S3}) + g_4\Theta^2 + g_5\Theta\tilde{\Theta} + g_6\tilde{\Theta}^2 = 0.\end{aligned}\quad (12)$$

And from Eq. (12), we can get the supersymmetric vacua for the fields $\Phi_S, \Theta, \tilde{\Theta}$

$$\langle \Phi_S \rangle = \frac{1}{\sqrt{2}} (v_S, v_S, v_S), \quad \langle \Theta \rangle = \frac{v_\Theta}{\sqrt{2}}, \quad \langle \tilde{\Theta} \rangle = 0, \quad \text{with } v_\Theta = v_S \sqrt{-3 \frac{g_3}{g_4}}, \quad (13)$$

where v_Θ is undetermined. As can be seen in Eq. (13), the VEVs v_Θ and v_S are naturally of the same order of magnitude (here the dimensionless parameters g_3 and g_4 are the same order of magnitude). Finally, the minimization equation for the vacuum configuration of Ψ is given by

$$\frac{\partial W_v}{\partial \Psi_0} = g_7(\Psi\tilde{\Psi} - \mu_\Psi^2) = 0, \quad (14)$$

where μ_Ψ is the $U(1)_X$ breaking scale and g_7 is a dimensionless coupling. From the above equation we can get the supersymmetric vacua for the fields $\Psi, \tilde{\Psi}$

$$\langle \Psi \rangle = \langle \tilde{\Psi} \rangle = \frac{v_\Psi}{\sqrt{2}}. \quad (15)$$

Note that, once the scale of breakdown of $U(1)_X$ symmetry is fixed, all the other scales of VEVs are determined by the present flavor structured model. As can be seen in Eqs. (13) and (15), in the SUSY limit there exist flat directions along which the scalar fields Φ_S, Θ and $\Psi, \tilde{\Psi}$ do not feel the potential. The SUSY-breaking effect lifts up the flat directions and corrects the VEV of the driving fields, leading to soft SUSY-breaking mass terms (here we do not specify a SUSY breaking mechanism in this work).

The flavon field \mathcal{F} charged under $U(1)_X$ is a scalar field which acquires a VEV and breaks spontaneously the flavored-PQ symmetry $U(1)_X$. In order to extract NG modes resulting from spontaneous breaking of $U(1)_X$ symmetry, we set the decomposition of complex scalar

fields as follows¹⁰

$$\begin{aligned}\Phi_{Si} &= \frac{e^{i\frac{\phi_S}{v_S}}}{\sqrt{2}} (v_S + h_S) , & \Theta &= \frac{e^{i\frac{\phi_\Theta}{v_\Theta}}}{\sqrt{2}} (v_\Theta + h_\Theta) , \\ \Psi &= \frac{v_\Psi}{\sqrt{2}} e^{i\frac{\phi_\Psi}{v_g}} \left(1 + \frac{h_\Psi}{v_g} \right) , & \tilde{\Psi} &= \frac{v_{\tilde{\Psi}}}{\sqrt{2}} e^{-i\frac{\phi_{\tilde{\Psi}}}{v_g}} \left(1 + \frac{h_{\tilde{\Psi}}}{v_g} \right) ,\end{aligned}\quad (16)$$

in which we have set $\Phi_{S1} = \Phi_{S2} = \Phi_{S3} \equiv \Phi_{Si}$ in the supersymmetric limit, and $v_g = \sqrt{v_\Psi^2 + v_{\tilde{\Psi}}^2}$. And the NG modes A_1 and A_2 are expressed as [2]

$$A_1 = \frac{v_S \phi_S + v_\Theta \phi_\Theta}{\sqrt{v_S^2 + v_\Theta^2}} , \quad A_2 = \phi_\Psi \quad (17)$$

with the angular fields ϕ_S , ϕ_Θ and ϕ_Ψ .

IV. QUARKS AND FLAVORED-AXIONS

Let us impose $SL_2(F_3) \times U(1)_X$ quantum numbers on SM quarks in a way that quark masses and mixings are well described as well as no axionic domain-wall problem occurs¹¹.

Under $SL_2(F_3) \times U(1)_X$, we assign the left-handed quark $SU(2)_L$ doublets denoted as Q_1 , Q_2 and Q_3 to the $(\mathbf{1}, 4p + 4q)$, $(\mathbf{1}', 2p + 2q)$ and $(\mathbf{1}'', 0)$, respectively, while the right-handed up-type quark $SU(2)_L$ singlets are assigned as $\mathcal{U}^c = \{u^c, c^c\}$ and t^c to the $(\mathbf{2}', -q - 2p)$ and $(\mathbf{1}', 0)$, respectively, and the right-handed down-type quarks $\mathcal{D}^c = \{d^c, s^c\}$ and b^c to the $(\mathbf{2}', -3q - 2p)$ and $(\mathbf{1}', -q)$, respectively. Under $SL_2(F_3) \times U(1)_X$ with $U(1)_R = +1$, the quantum numbers of the SM quark fields are summarized as in Table II. The $U(1)_X$ invari-

TABLE II: Representations of the quark fields under $SL_2(F_3) \times U(1)_X$ with $U(1)_R = +1$.

Field	Q_1, Q_2, Q_3	\mathcal{D}^c, b^c	\mathcal{U}^c, t^c
$SL_2(F_3)$	$\mathbf{1}, \mathbf{1}', \mathbf{1}''$	$\mathbf{2}', \mathbf{1}'$	$\mathbf{2}', \mathbf{1}'$
$U(1)_X$	$4p + 4q, 2p + 2q, 0$	$-3q - 2p, -q$	$-q - 2p, 0$

ance forbids renormalizable Yukawa couplings for the light families, but would allow them through effective nonrenormalizable couplings suppressed by $(\mathcal{F}/\Lambda)^n$ with some positive integer n . Here Λ , above which there exists unknown physics, is the scale of flavor dynamics,

¹⁰ Note that the massless modes are not contained in the $\tilde{\Theta}, \Phi_0^S, \Theta_0$ fields in supersymmetric limit.

¹¹ See Appendix D.

and is associated with heavy states which are integrated out. The Yukawa superpotential for quark sector invariant under $G_{\text{SM}} \times G_F \times U(1)_R$ is given by

$$\begin{aligned}
W_q = & \hat{y}_t t^c Q_3 H_u + y_c (\eta \mathcal{U}^c)_{1''} Q_2 \frac{H_u}{\Lambda} + y_u [(\eta \mathcal{U}^c)_{\mathbf{3}} \Phi_S]_1 Q_1 \frac{H_u}{\Lambda^2} \\
& + y_b b^c Q_3 H_d + y_s (\eta \mathcal{D}^c)_{1''} Q_2 \frac{H_d}{\Lambda} + Y_s b^c Q_2 (\Phi_S \Phi_T)_{1'} \frac{H_d}{\Lambda^2} + y_d [(\eta \mathcal{D}^c)_{\mathbf{3}} \Phi_S]_1 Q_1 \frac{H_d}{\Lambda^2} \\
& + Y_d b^c Q_1 (\Phi_S \Phi_S)_{1''} \frac{H_d}{\Lambda^2} + \tilde{y}_d [(\eta \mathcal{D}^c)_{\mathbf{3}} \Phi_T]_1 Q_1 \frac{H_d}{\Lambda^2}, \tag{18}
\end{aligned}$$

where the hat Yukawa coupling denotes order of unity *i.e.*, $1/\sqrt{10} \lesssim |\hat{y}| \lesssim \sqrt{10}$, and

$$\begin{aligned}
y_c = \hat{y}_c \left(\frac{\Psi}{\Lambda} \right), \quad y_u = \hat{y}_u \left(\frac{\Psi}{\Lambda} \right)^3, \quad y_b = \hat{y}_b \left(\frac{\tilde{\Psi}}{\Lambda} \right), \quad y_s = \hat{y}_s \left(\frac{\tilde{\Psi}}{\Lambda} \right) \\
Y_s = \hat{Y}_s \left(\frac{\Psi}{\Lambda} \right), \quad y_d = \hat{y}_d \left(\frac{\Psi}{\Lambda} \right), \quad Y_d = \hat{Y}_d \left(\frac{\Psi}{\Lambda} \right)^3, \quad \tilde{y}_d = \hat{\tilde{y}}_d \left(\frac{\Psi}{\Lambda} \right) \left(\frac{\Theta}{\Lambda} \right). \tag{19}
\end{aligned}$$

Higher dimensional operators driven by Φ_T and η fields, *e.g.* $\tilde{y}_c [(\eta \mathcal{U}^c)_{\mathbf{3}} \Phi_T]_{1''} Q_2 \frac{H_u}{\Lambda^2}$ with $\tilde{y}_c = \hat{\tilde{y}}_c (\Psi/\Lambda)$ is neglected here, but will be included in numerical calculation.

Once the scalar fields $\Phi_S, \Theta, \tilde{\Theta}, \Psi$ and $\tilde{\Psi}$ get VEVs, the flavored $U(1)_X$ symmetry is spontaneously broken¹². And at energies below the electroweak scale, all quarks and leptons obtain masses. The relevant quark interaction terms with chiral fermions is given by

$$-\mathcal{L}_{WY}^q = \overline{q_R^u} \mathcal{M}_u q_L^u + \overline{q_R^d} \mathcal{M}_d q_L^d + \frac{g}{\sqrt{2}} W_\mu^+ \overline{q_L^u} \gamma^\mu q_L^d + \text{h.c.}, \tag{20}$$

where $q^u = (u, c, t)$, $q^d = (d, s, b)$, and g is the $SU(2)$ coupling constant. With the desired direction of Eqs. (11, 13, 15)¹³ the up(down)-type quark mass matrices in the above Lagrangian (20) read¹⁴

$$\begin{aligned}
\mathcal{M}_u = & \begin{pmatrix} i y_u \nabla_\eta \nabla_S e^{i(\frac{A_1}{v_{\mathcal{F}}} + 3\frac{A_2}{v_g})} & 0 & 0 \\ \frac{1-i}{2} y_u \nabla_\eta \nabla_S e^{i(\frac{A_1}{v_{\mathcal{F}}} + 3\frac{A_2}{v_g})} & y_c \nabla_\eta e^{i\frac{A_2}{v_g}} & 0 \\ 0 & 0 & \hat{y}_t \end{pmatrix} v_u, \\
\mathcal{M}_d = & \begin{pmatrix} (i y_d \nabla_S + \tilde{y}_d \nabla_T) \nabla_\eta e^{i(\frac{A_1}{v_{\mathcal{F}}} + \frac{A_2}{v_g})} & 0 & 0 \\ \frac{1-i}{2} y_d \nabla_\eta \nabla_S e^{i(\frac{A_1}{v_{\mathcal{F}}} + \frac{A_2}{v_g})} & y_s \nabla_\eta e^{-i\frac{A_2}{v_g}} & 0 \\ 3 Y_d \nabla_S^2 e^{i(2\frac{A_1}{v_{\mathcal{F}}} + 3\frac{A_2}{v_g})} & Y_s \nabla_T \nabla_S e^{i(\frac{A_1}{v_{\mathcal{F}}} + \frac{A_2}{v_g})} & y_b e^{-i\frac{A_2}{v_g}} \end{pmatrix} v_d, \tag{21}
\end{aligned}$$

¹² If the symmetry $U(1)_X$ is broken spontaneously, the massless modes A_1 of the scalar Φ_S (and/or Θ) and A_2 of the scalar $\Psi(\tilde{\Psi})$ appear as phases.

¹³ Here we took $\langle \eta \rangle = \frac{v_\eta}{\sqrt{2}}(+1, 0)$.

¹⁴ Even there seem to have vacuum corrections to the leading order picture in Eq.(21), *e.g.* $-\hat{y}_s \frac{\delta v_{\eta_2}}{\Lambda} \nabla_\Psi d^c Q_2 H_d$ and $-\hat{y}_c \frac{\delta v_{\eta_2}}{\Lambda} \nabla_\Psi u^c Q_2 H_u$, by the higher-dimensional operators in the driving superpotential Eq. (B4), one can make their contributions vanishing or small enough.

where $\langle H_u \rangle \equiv v_u = v \sin \beta / \sqrt{2}$ and $\langle H_d \rangle \equiv v_d = v \cos \beta / \sqrt{2}$ with $v = 246$ GeV, $v_{\mathcal{F}} = v_{\Theta}(1 + \kappa^2)^{1/2}$ with $\kappa = v_S/v_{\Theta}$ in SUSY limit, and

$$\nabla_Q \equiv \frac{v_Q}{\sqrt{2}\Lambda} \quad \text{with } Q = \eta, S, T, \Theta, \Psi. \quad (22)$$

Here $\mathcal{M}_f = V_R^{f\dagger} \text{Diag}(m_{f_1}, m_{f_2}, m_{f_3}) V_L^f$ where f_i stands for i -th generation of f -type quark, and V_L^f and V_R^f are the diagonalization matrices for $\mathcal{M}_f^\dagger \mathcal{M}_f$ and $\mathcal{M}_f \mathcal{M}_f^\dagger$, respectively. One of the most interesting features observed by experiments on the quarks is that the mass spectrum of the up-type quarks exhibits a much stronger hierarchical pattern to that of the down-type quarks, which may indicate that the CKM matrix [26] is mainly generated by the mixing matrix of the down-type quark sector. So the following *new* expansion parameters could be defined in a way that the diagonalizing matrices V_L^d and V_L^u satisfy the CKM matrix in the Wolfenstein parametrization $V_{\text{CKM}} = V_L^u V_L^{d\dagger}$:

$$\nabla_T = \kappa \frac{|\hat{y}_d|}{|\hat{\bar{y}}_d|} \quad \text{with } \phi_{\bar{d}} = -\phi_d - \frac{\pi}{2}, \quad (23)$$

$$\nabla_{\Psi} \simeq \lambda^{3/4} \left| \frac{X_1 \delta_2^G}{X_2 \delta_1^G} \right|^{\frac{1}{2}} \left(\frac{B(1 + \kappa^2)}{6\kappa^2} \frac{|\hat{y}_b|}{|\hat{Y}_d|} \right)^{\frac{1}{4}}, \quad (24)$$

$$\nabla_{\Theta} = \frac{1}{\kappa} \nabla_S = \left| \frac{X_2 \delta_1^G}{X_1 \delta_2^G} \right| \sqrt{\frac{2}{1 + \kappa^2}} \nabla_{\Psi}, \quad (25)$$

where $\arg(\hat{y}_i) \equiv \phi_i$ and $B = A\sqrt{\rho^2 + \eta^2}$ with the Wolfenstein parametrization¹⁵ (λ, ρ, η, A) [25]. Note that the expansion parameters ∇_{Ψ} and $\nabla_{\Theta}(\nabla_S)$ associated with the $U(1)_X$ charged fields are defined by the relation Eq. (3) associated with the two QCD anomalous $U(1)$, containing the model dependent parameter $|X_i \delta_j^G / X_j \delta_i^G|$ with $i \neq j$.

From the empirical down-type quark mass ratios calculated from the measured values $(m_d/m_b)_{\text{PDG}} \doteq 1.12_{-0.11}^{+0.13} \times 10^{-3}$ and $(m_s/m_b)_{\text{PDG}} \doteq 2.30_{-0.12}^{+0.21} \times 10^{-2}$ with $(m_b)_{\text{PDG}} \doteq 4.18_{-0.03}^{+0.04}$ GeV [26], we can obtain roughly the down-type quark mixing angles in the standard parametrization [27]

$$\theta_{12}^d \approx \frac{1}{\sqrt{2}} \left| \frac{\hat{y}_d}{\hat{y}_s} \right| \nabla_S, \quad \theta_{23}^d \simeq \left| \frac{\hat{Y}_s}{\hat{y}_b} \right| \nabla_S \nabla_T^2, \quad \theta_{13}^d \simeq 3 \left| \frac{\hat{Y}_d}{\hat{y}_b} \right| \nabla_{\Psi}^2 \nabla_S^2. \quad (26)$$

And their corresponding down-type quark masses are roughly given by

$$m_d \simeq 2|\hat{y}_d| \nabla_{\Psi} \nabla_S \nabla_{\eta} |\sin \phi_d| v_d, \quad m_s \simeq |\hat{y}_s| \nabla_{\Psi} \nabla_{\eta} v_d, \quad m_b \simeq |\hat{y}_b| \nabla_{\Psi} v_d. \quad (27)$$

¹⁵ We take $\lambda = 0.22509_{-0.00071}^{+0.00091}$, $A = 0.825_{-0.037}^{+0.020}$, $\bar{\rho} = \rho/(1 - \lambda^2/2) = 0.160_{-0.021}^{+0.034}$, and $\bar{\eta} = \eta/(1 - \lambda^2/2) = 0.350_{-0.024}^{+0.024}$ with 3σ errors [28].

Note that the parametrization of Eq. (23) is very crucial to reproduce the d - and s -quark mass and the mixing angle θ_{12}^d .

From the mass ratio of t - and b -quark $(m_b/m_t)_{\text{PDG}} \doteq 2.41_{-0.03}^{+0.03} \times 10^{-2}$ in PDG [26] the value of $\tan \beta \equiv v_u/v_d$ can be obtained in a good approximation:

$$\tan \beta \simeq \lambda^{\frac{3}{2}} \left(\frac{m_t}{m_b} \right)_{\text{PDG}} \left| \frac{\hat{y}_b}{\hat{y}_t} \right| \left| \frac{X_1 \delta_2^G}{X_2 \delta_1^G} \right| \left(\frac{B(1 + \kappa^2)}{6\kappa^3} \left| \frac{\hat{y}_b}{\hat{Y}_d} \right| \right)^{\frac{1}{2}}. \quad (28)$$

The top Yukawa coupling \hat{y}_t can be directly obtained from the top quark mass $m_t = |\hat{y}_t|v_u = 173.1 \pm 0.6 \text{ GeV}$ [26]. From the hierarchical mass ration between u - and c -quark $(m_u/m_c)_{\text{PDG}} \doteq 1.72_{-0.34}^{+0.52} \times 10^{-3}$ we obtain

$$\left(\frac{m_u}{m_c} \right)_{\text{PDG}} \simeq \sqrt{\frac{3}{2}} \left| \frac{\hat{y}_u}{\hat{y}_c} \right| \nabla_\Psi^2 \nabla_S, \quad (29)$$

and its corresponding mixing angle

$$\theta_{12}^u \simeq \frac{1}{\sqrt{2}} \left| \frac{\hat{y}_u}{\hat{y}_c} \right| \nabla_S \nabla_\Psi^2. \quad (30)$$

In turn, the expansion parameter ∇_η is defined by using $(m_c/m_t)_{\text{PDG}} \doteq 7.39_{-0.20}^{+0.20} \times 10^{-3}$:

$$\nabla_\eta \simeq \lambda^{\frac{13}{4}} \left| \frac{X_2 \delta_1^G}{X_1 \delta_2^G} \right|^{\frac{1}{2}} \left| \frac{\hat{y}_t}{\hat{y}_c} \right| \left(\frac{426 \kappa^2}{B(1 + \kappa^2)} \left| \frac{\hat{Y}_d}{\hat{y}_b} \right| \right)^{\frac{1}{4}}. \quad (31)$$

As designed, with the fields redefinition the CKM matrix with $J_{CP}^{\text{quark}} = \text{Im}[V_{us}V_{cb}V_{ub}^*V_{cs}^*] \simeq A^2\lambda^6\sqrt{\rho^2 + \eta^2} \sin \delta_{CP}^q$ and its CP phase $\delta_{CP}^q \equiv \phi_2^d - 2\phi_3^d = \tan^{-1}(\eta/\rho)$ is well described, where $\phi_2^d \simeq \arg(\hat{Y}_d^*\hat{y}_b) - \phi_1^d/2$ and $2\phi_3^d \simeq \arg(\hat{Y}_d^*\hat{y}_b) + \phi_1^d - \phi_2^d$, and $\phi_1^d = \arg(\hat{Y}_s^*\hat{y}_b)/2$.

Hence it is very crucial for obtaining the right values of the new expansion parameters to reproduce the empirical results of the CKM mixing angles and quark masses. In addition, such right values are needed to reproduce the empirical results of the charged leptons and the light active neutrino masses in our model. In the following subsequent section we will perform a numerical simulation.

A. Numerical analysis for Quark sector

We perform a numerical simulation¹⁶ using the linear algebra tools of Ref. [29]. With the inputs

$$\tan \beta = 7.40, \quad \kappa = 0.96, \quad (32)$$

and $|\hat{y}_d| = 0.9200$ ($\phi_d = 6.2100$ rad), $|\hat{\tilde{y}}_d| = 3.1400$, $|\hat{y}_s| = 0.3300$ ($\phi_s = 2.9300$ rad), $|\hat{y}_b| = 1.0100$ ($\phi_b = 0$), $|\hat{y}_u| = 0.3300$ ($\phi_u = 0$ rad), $|\hat{y}_c| = 0.4400$ ($\phi_c = 5.9700$ rad), $|\hat{\tilde{y}}_c| = 0.8040$ ($\phi_{\tilde{c}} = 5.9900$ rad), $|\hat{y}_t| = 1.0042$ ($\phi_t = 0$), $|\hat{Y}_d| = 2.8000$ ($\phi_{Y_d} = 2.6000$ rad), $|\hat{Y}_s| = 1.3200$ ($\phi_{Y_s} = 5.1900$ rad), leading to

$$\nabla_\Psi = 0.1770, \quad \nabla_S = 0.1156, \quad \nabla_T = 0.2813, \quad \nabla_\eta = 0.0740, \quad (33)$$

we obtain the mixing angles and Dirac CP phase $\theta_{12}^q = 12.9930^\circ$, $\theta_{23}^q = 2.4339^\circ$, $\theta_{13}^q = 0.2018^\circ$, $\delta_{CP}^q = 64.9888^\circ$ compatible with the 3σ Global fit of CKMfitter [28]; the masses $m_d = 4.6244$ MeV, $m_s = 102.8420$ MeV, $m_b = 4.1682$ GeV, $m_u = 2.6977$ MeV, $m_c = 1.2785$ GeV, and $m_t = 173.1$ GeV.

Below the scale of spontaneous $SU(2)_L \times U(1)_Y$ gauge symmetry breaking, the running mass includes corrections from QCD and QED loops [26]. In order to explain the experimental data on quark and lepton masses¹⁷ we have used, it is meaningful to use the masses at a common momentum scale μ which is heavier than the QCD scale of about 1 GeV. Hence, in the $\overline{\text{MS}}$ scheme for the light quark (u -, d -, and s -quark) the renormalization scale has been chosen to be a common scale $\mu \approx 2$ GeV and their masses are current quark masses at $\mu \approx 2$ GeV, and for heavy quarks (b - and c -quark) the renormalization scale equal to the quark mass are chosen to be $\bar{m}_Q(\mu)$ at $\mu = \bar{m}_Q$. For top quark (t -quark), the t -quark mass at scales below the pole mass is unphysical since the t -quark decouples at its scale, hence its mass is more directly determined by experiments, see Ref. [26], leading to the value we have used.

¹⁶ Here, in numerical calculation, we have only considered the mass matrices in Eq. (21) since it is expected that the corrections to the VEVs due to dimensional operators contributing to Eq. (7) could be small enough below a few percent level, see Appendix B.

¹⁷ For charged leptons (e, μ, τ) we have used the experimental data [26] in this work since the difference between pole mass and running mass are less significant.

B. Scale of PQ phase transition induced by Hadron sector

In order to obtain the QCD axion decay constant F_A (or, equivalently, flavored-axion decay constants $F_{a_i} = f_{a_i}/\delta_i^G$ through flavored-axion model[2]), we consider here two constraints coming from the astroparticle physics, *e.g.* axion cooling of stars[17, 21, 30–32], and flavor-violating processes induced by the flavored-axions, *e.g.* $K^+ \rightarrow \pi^+ + A_i$, etc.[13, 14, 16, 33, 34].

(i) Below the chiral symmetry breaking scale, the axion-hadron interactions are meaningful for the axion production rate in the core of a star where the temperature is not as high as 1 GeV, which is given by

$$-\mathcal{L}^{a-\psi_N} = \frac{\partial_\mu a}{2F_A} X_{\psi_N} \bar{\psi}_N \gamma_\mu \gamma^5 \psi_N \quad (34)$$

where the QCD axion decay constant is given by $F_A = f_A/N$ with $f_A = \sqrt{2}\delta_2^G f_{a_1} = \sqrt{2}\delta_1^G f_{a_2}$, and ψ_N is the nucleon doublet $(p, n)^T$ (here p and n correspond to the proton field and neutron field, respectively). The couplings of the axion to the nucleon can be rewritten as[2]

$$-\mathcal{L}_A \supset \frac{\partial^\mu a}{2F_A} \left\{ \left(\frac{\tilde{X}_u}{N} - \frac{1}{1+z+\omega} \right) \bar{u} \gamma^\mu \gamma_5 u + \left(\frac{\tilde{X}_d}{N} - \frac{z}{1+z+\omega} \right) \bar{d} \gamma^\mu \gamma_5 d \right. \\ \left. + \left(\frac{\tilde{X}_s}{N} - \frac{\omega}{1+z+\omega} \right) \bar{s} \gamma^\mu \gamma_5 s \right\}, \quad (35)$$

where $\tilde{X}_q = \delta_2^G X_{1q} + \delta_1^G X_{2q}$ with $q = u, d, s$ and $X_{1u} = 8$, $X_{1d} = 8$, $X_{1s} = 0$, $X_{2u} = 3$, $X_{2d} = 1$, $X_{2s} = -1$. From Eqs.(34-35) the QCD axion coupling to the neutron can be obtained as

$$g_{Ann} = \frac{X_n m_n}{F_A}, \quad (36)$$

where the neutron mass $m_n = 939.6$ MeV, and the axion-neutron coupling, X_n , related to axial-vector current matrix elements by Goldberger-Treiman relations[26] is obtained as

$$X_n = \left(\frac{3}{4} - \eta \right) \Delta d + \left(\frac{5}{12} - \eta z \right) \Delta u - \left(\frac{1}{6} + \eta \omega \right) \Delta s, \quad (37)$$

where $\eta = (1+z+\omega)^{-1}$ with $z = m_u/m_d$ and $\omega = m_u/m_s \ll z$, and the Δq are given by the axial vector current matrix element $\Delta q S_\mu = \langle p | \bar{q} \gamma_\mu \gamma^5 q | p \rangle$. Now, for numerical estimations on Eq.(36) we adopt the central values of $\Delta u = 0.84 \pm 0.02$, $\Delta d = -0.43 \pm 0.02$ and

$\Delta s = -0.09 \pm 0.02$, and take the Weinberg value for $0.38 < z < 0.58$ [26] and $\omega = 0.315 z$. Then, the value of the axion-neutron coupling lies in ranges $0.007 \lesssim X_n \lesssim 0.111$. There is a hint for extra cooling from the neutron star in the supernova remnant “Cassiopeia A” by axion neutron bremsstrahlung, requiring a coupling to the neutron of size $g_{Ann} = (3.8 \pm 3) \times 10^{-10}$ [31], which is translated into $9.94 \times 10^6 \lesssim F_A/\text{GeV} \lesssim 1.31 \times 10^9$. However, since the cooling of the superfluid core in the neutron star can also be explained by neutrino emission in pair formation in a multicomponent superfluid state ${}^3\text{P}_2(m_j = 0, \pm 1, \pm 2)$ [30], one may not take it seriously. The range quoted is compatible with the state-of-the-art upper limit on the coupling from neutron star cooling $g_{Ann} < 8 \times 10^{-10}$ [21], whose upper bound is interpreted as the lower bound of the QCD axion decay constant:

$$F_A > (0.84 - 13.08) \times 10^7 \text{ GeV}. \quad (38)$$

(ii) Since a direct interaction of the SM gauge singlet flavon fields charged under $U(1)_X$ with the SM quarks charged under $U(1)_X$ can arise through Yukawa interaction, the flavored-axion interactions with the flavor violating coupling to the s - and d -quark is given by

$$\mathcal{L}_Y^{A_i s d} \simeq i \left(\frac{|X_1| A_1}{2f_{a_1}} + \frac{|X_2| A_2}{f_{a_2}} \right) \bar{s} d (m_s - m_d) \lambda \left(1 - \frac{\lambda^2}{2} \right), \quad (39)$$

where¹⁸ $V_L^{d\dagger} \approx V_{\text{CKM}}$, $f_{a_1} = |X_1| v_{\mathcal{F}}$, and $f_{a_2} = |X_2| v_g$ are used. Then the decay width of $K^+ \rightarrow \pi^+ + A_i$ is given by [11, 14, 15]

$$\Gamma(K^+ \rightarrow \pi^+ + A_i) = \frac{m_K^3}{16\pi} \left(1 - \frac{m_\pi^2}{m_K^2} \right)^3 |\mathcal{M}_{dsi}|^2, \quad (40)$$

where $m_{K^\pm} = 493.677 \pm 0.013 \text{ MeV}$, $m_{\pi^\pm} = 139.57018(35) \text{ MeV}$ [26], and

$$|\mathcal{M}_{ds1}|^2 = \left| \frac{1}{f_{a_1}/k_2} \lambda \left(-1 + \frac{\lambda^2}{2} \right) \right|^2, \quad |\mathcal{M}_{ds2}|^2 = \left| \frac{1}{f_{a_2}/k_1} \lambda \left(-1 + \frac{\lambda^2}{2} \right) \right|^2. \quad (41)$$

From the present experimental upper bound $\text{Br}(K^+ \rightarrow \pi^+ A_i) < 7.3 \times 10^{-11}$ [16] with $\text{Br}(K^+ \rightarrow \pi^+ \nu \bar{\nu}) = 1.73_{-1.05}^{+1.15} \times 10^{-10}$ [33], we obtain the lower limits of flavored-axion decay constants and their corresponding QCD axion decay constant

$$\begin{aligned} f_{a_1} > |k_2| \times 1.15 \times 10^{11} \text{ GeV} & \Leftrightarrow F_A = \frac{f_{a_1}}{4|k_2|\sqrt{2}} > 2.03 \times 10^{10} \text{ GeV} \\ f_{a_2} > |k_1| \times 1.15 \times 10^{11} \text{ GeV} & \Leftrightarrow F_A = \frac{f_{a_2}}{3|k_1|\sqrt{2}} > 2.72 \times 10^{10} \text{ GeV} \end{aligned}, \quad (42)$$

¹⁸ Actually, in the standard parametrization the mixing elements of V_R^d are given by $\theta_{23}^R \simeq A\lambda^2 \nabla_\eta |\hat{y}_s/\hat{y}_b|$, $\theta_{13}^R \simeq \sqrt{2} B \lambda^3 \nabla_\eta \nabla_S$, and $\theta_{12}^R \simeq \sqrt{2} |\hat{y}_d/\hat{y}_s|^2 \cos \phi_{\tilde{d}} \nabla_S^2$. Its effect to the flavor violating coupling to the s - and d -quark is negligible: $(V_R^d \text{Diag.}(\frac{A_1}{v_{\mathcal{F}}} + \frac{2A_2}{v_g}, \frac{A_1}{v_{\mathcal{F}}} + \frac{2A_2}{v_g}, 0) V_R^{d\dagger})_{12} = 0$ at leading order.

where $F_A = f_{a_i}/(\delta_i^G \sqrt{2})$ is used. Note that the lower bounds of flavored-axion decay constants f_{a_i} are dependent on the values of k_i , while the QCD axion decay constant F_A does depend on the properties (2α and ω in Eq. (6)) from the QCD instanton background instead of the k_i . Clearly, from Eqs. (38) and (42) the most stringent constraint on the QCD axion decay constant comes from the present experimental upper bound $\text{Br}(K^+ \rightarrow \pi^+ A_i) < 7.3 \times 10^{-11}$ [16]

$$F_A > 2.72 \times 10^{10} \text{ GeV}. \quad (43)$$

In the near future the NA62 experiment will be expected to reach the sensitivity of $\text{Br}(K^+ \rightarrow \pi^+ + A_i) < 1.0 \times 10^{-12}$ [13], which is interpreted as the flavored-axion decay constant and its corresponding QCD axion decay constant

$$f_{a_i} > 9.86 \times 10^{11} \text{ GeV} \Leftrightarrow F_A > 2.32 \times 10^{11} \text{ GeV}. \quad (44)$$

V. LEPTONS AND FLAVORED-AXIONS

Next, we assign the left-handed charged lepton $SU(2)_L$ doublets denoted as L_e, L_μ, L_τ to the $(\mathbf{1}, -p - \mathcal{Q}_{y_1^\nu}), (\mathbf{1}', -p - \mathcal{Q}_{y_1^\nu}),$ and $(\mathbf{1}'', -p - \mathcal{Q}_{y_1^\nu}),$ respectively, while the right-handed charged leptons denoted as e^c, μ^c and τ^c , the electron flavor to the $(\mathbf{1}, p + \mathcal{Q}_{y_1^\nu} + 6q),$ the muon flavor to the $(\mathbf{1}'', p + \mathcal{Q}_{y_1^\nu} - 3q),$ and the tau flavor to the $(\mathbf{1}', p + \mathcal{Q}_{y_1^\nu} - q).$ And we assign the right-handed neutrinos $SU(2)_L$ singlets denoted as N^c to the $(\mathbf{3}, p).$ Note that $\mathcal{Q}_{y_1^\nu} = \mathcal{Q}_{y_2^\nu} = \mathcal{Q}_{y_3^\nu}$ is assigned to give a tribimaximal (TBM)-like mixing pattern. In addition, additional Majorana fermions are introduced to have no axionic domain-wall problem, which link low energy neutrino oscillations to astronomical-scale baseline neutrino oscillations. Under $SL_2(F_3) \times U(1)_X$ we assign the additional Majorana neutrinos $SU(2)_L$ singlets denoted as S_e^c, S_μ^c and S_τ^c to the $(\mathbf{1}, p + \mathcal{Q}_{y_1^\nu} - \mathcal{Q}_{y_1^s}), (\mathbf{1}'', p + \mathcal{Q}_{y_1^\nu} - \mathcal{Q}_{y_2^s})$ and $(\mathbf{1}', p + \mathcal{Q}_{y_1^\nu} - \mathcal{Q}_{y_3^s}),$ respectively. Here \mathcal{Q}_Y denotes the $U(1)_X$ quantum number of Yukawa coupling \mathcal{Y} which appears in the superpotentials (18) and (45) sewed by the five (among seven) in-equivalent representations $\mathbf{1}, \mathbf{1}', \mathbf{1}'', \mathbf{2}'$ and $\mathbf{3}$ of $SL_2(F_3).$

As mentioned before, with the conditions (4) and (D4) satisfied, new additional Majorana fermions $S_{e, \mu, \tau}^c$ besides the heavy Majorana neutrinos are introduced in the lepton sector. Hence, such new additional Majorana neutrinos can play a role of the active neutrinos as pseudo-Dirac neutrinos. Under $SL_2(F_3) \times U(1)_X$ with $U(1)_R = +1,$ the quantum numbers of

the lepton fields are summarized as in Table III. The lepton Yukawa superpotential, similar

TABLE III: Representations of the lepton fields under $SL_2(F_3) \times U(1)_X$ with $U(1)_R = +1$. And here $r \equiv Q_{y_1^\nu} + p$ is defined.

Field	L_e, L_μ, L_τ	e^c, μ^c, τ^c	N^c	S_e^c, S_μ^c, S_τ^c
$SL_2(F_3)$	1, 1', 1''	1, 1'', 1'	3	1, 1'', 1'
$U(1)_X$	$-r$	$r - Q_{y_e}, r - Q_{y_\mu}, r - Q_{y_\tau}$	p	$r - Q_{y_1^s}, r - Q_{y_2^s}, r - Q_{y_3^s}$

to the quark sector, invariant under $G_{\text{SM}} \times G_F \times U(1)_R$ reads

$$\begin{aligned}
W_{\ell\nu} = & y_\tau \tau^c L_\tau H_d + y_\mu \mu^c L_\mu H_d + y_e e^c L_e H_d \\
& + y_1^s S_e^c L_e H_u + y_2^s S_\mu^c L_\mu H_u + y_3^s S_\tau^c L_\tau H_u \\
& + \left\{ y_1^\nu (N^c \Phi_T)_1 L_e + y_2^\nu (N^c \Phi_T)_{1'} L_\mu + y_3^\nu (N^c \Phi_T)_{1'} L_\tau \right\} \frac{H_u}{\Lambda} \\
& + \frac{1}{2} (\hat{y}_\Theta \Theta + \hat{y}_{\tilde{\Theta}} \tilde{\Theta}) (N^c N^c)_1 + \frac{\hat{y}_R}{2} (N^c N^c)_3 \Phi_S \\
& + \frac{1}{2} \{ y_1^{ss} S_e^c S_e^c + y_2^{ss} S_\mu^c S_\mu^c + y_3^{ss} S_\tau^c S_\tau^c \} \Theta.
\end{aligned} \tag{45}$$

Remark that, as in the SM quark fields since the $U(1)_X$ quantum numbers are arranged to lepton fields as in Table III with the conditions (4) and (D4) satisfied, it is expected that the SM gauge singlet flavon fields derive higher-dimensional operators, which are eventually visualized into the Yukawa couplings of leptons as a function of flavon fields $\Psi(\tilde{\Psi})$.

For pseudo-Dirac neutrino as the active neutrino to be realized in a way that the neutrino oscillations at low energies could have a direct connection to new neutrino oscillations available on high-energy neutrinos [2], two requirements are needed since the quantum numbers $L_{e,\mu,\tau}$ (or equivalently $Q_{y_i^\nu}$) are not uniquely determined: (i) the quantum numbers $Q_{y_i^\nu}$ and $Q_{y_i^s}$ should have opposite sign due to $Q_{y_1^{ss}} = 2(Q_{y_1^s} - Q_{y_1^\nu})$ and $Q_{y_2^{ss}} = Q_{y_3^{ss}} = Q_{y_2^s} + Q_{y_3^s} - 2Q_{y_1^\nu}$, (ii) especially, the quantum numbers $Q_{y_2^s}$ and $Q_{y_3^s}$ should have the same sign for normal neutrino mass ordering, and (iii)

$$|Q_{y_i^{ss}}| \gg |Q_{y_i^s}| \gg |Q_{y_i^\nu}|, \tag{46}$$

As we shall see later, it could make a connection between the neutrino oscillation at low energies and new oscillations available on high-energy neutrinos through astronomical-scale baseline. Then, the quantum numbers $Q_{y_i^s}$ can be uniquely determined by taking into

account both the $U(1)_X \times [\text{gravity}]^2$ anomaly-free condition in Eq. (D5) and the hat Yukawa coupling of order unity, $1/\sqrt{10} \lesssim |\hat{y}_i^s| \lesssim \sqrt{10}$, we obtain (i) $|\mathcal{Q}_{y_3^s}| \gg |\mathcal{Q}_{y_1^s}| \geq |\mathcal{Q}_{y_2^s}|$ for inverted mass ordering (IO), and (ii) $|\mathcal{Q}_{y_1^s}| \gg |\mathcal{Q}_{y_2^s}| \geq |\mathcal{Q}_{y_3^s}|$ for normal mass ordering (NO). In such case, considering the observed neutrino mass hierarchy $\Delta m_{\text{sol}}^2 \equiv m_{\nu_2}^2 - m_{\nu_1}^2 \simeq 7.50 \times 10^{-5} \text{ eV}^2$ and $\Delta m_{\text{atm}}^2 \simeq 2.52 \times 10^{-3} \text{ eV}^2$ where $\Delta m_{\text{atm}}^2 \equiv m_{\nu_3}^2 - m_{\nu_1}^2$ for NO; $|m_{\nu_2}^2 - m_{\nu_3}^2|$ for IO, we have the followings:

For the case-I with $E/N = 3.83$ in Eq. (D3) the Yukawa couplings of charged-leptons are represented with $\mathcal{Q}_{y_\tau} = -q$, $\mathcal{Q}_{y_\mu} = 3q$, $\mathcal{Q}_{y_e} = -6q$ as

$$y_e = \hat{y}_e \left(\frac{\Psi}{\Lambda} \right)^6, \quad y_\mu = \hat{y}_\mu \left(\frac{\tilde{\Psi}}{\Lambda} \right)^3, \quad y_\tau = \hat{y}_\tau \left(\frac{\Psi}{\Lambda} \right); \quad (47)$$

the $U(1)_X$ quantum numbers of Yukawa couplings of pseudo-Dirac neutrinos are given for $k_1 = +k_2 = 1$ in Eq. (D6) as

$$\begin{aligned} \mathcal{Q}_{y_1^s} &= 63q, & \mathcal{Q}_{y_2^s} &= -18q, & \mathcal{Q}_{y_3^s} &= -17q & ; & \text{NO} \\ \mathcal{Q}_{y_1^s} &= \mp 17q, & \mathcal{Q}_{y_2^s} &= \pm 17q, & \mathcal{Q}_{y_3^s} &= 28q & ; & \text{IO} \end{aligned} \quad (48)$$

Here for NO the quantum numbers $\mathcal{Q}_{y_2^s}$ and $\mathcal{Q}_{y_3^s}$ should have the same sign, while for IO $\mathcal{Q}_{y_1^s}$ and $\mathcal{Q}_{y_2^s}$ should have the opposite sign.

For the case-II with $E/N = 3.16$ in Eq. (D3) the Yukawa couplings of charged-leptons are represented with $\mathcal{Q}_{y_\tau} = q$, $\mathcal{Q}_{y_\mu} = 3q$, $\mathcal{Q}_{y_e} = -6q$ as

$$y_e = \hat{y}_e \left(\frac{\Psi}{\Lambda} \right)^6, \quad y_\mu = \hat{y}_\mu \left(\frac{\tilde{\Psi}}{\Lambda} \right)^3, \quad y_\tau = \hat{y}_\tau \left(\frac{\tilde{\Psi}}{\Lambda} \right); \quad (49)$$

the $U(1)_X$ quantum numbers of Yukawa couplings of pseudo-Dirac neutrinos are given for $k_1 = +k_2 = 1$ in Eq. (D6) as

$$\begin{aligned} \mathcal{Q}_{y_1^s} &= 61q, & \mathcal{Q}_{y_2^s} &= -18q, & \mathcal{Q}_{y_3^s} &= -17q & ; & \text{NO} \\ \mathcal{Q}_{y_1^s} &= \mp 17q, & \mathcal{Q}_{y_2^s} &= \pm 17q, & \mathcal{Q}_{y_3^s} &= 26q & ; & \text{IO} \end{aligned} \quad (50)$$

For the case-III with $E/N = 1.83$ in Eq. (D3) the Yukawa couplings of charged-leptons are represented with $\mathcal{Q}_{y_\tau} = -q$, $\mathcal{Q}_{y_\mu} = -3q$, $\mathcal{Q}_{y_e} = 6q$ as

$$y_e = \hat{y}_e \left(\frac{\tilde{\Psi}}{\Lambda} \right)^6, \quad y_\mu = \hat{y}_\mu \left(\frac{\Psi}{\Lambda} \right)^3, \quad y_\tau = \hat{y}_\tau \left(\frac{\Psi}{\Lambda} \right); \quad (51)$$

the $U(1)_X$ quantum numbers of Yukawa couplings of pseudo-Dirac neutrinos are given for $k_1 = +k_2 = 1$ in Eq. (D6) as

$$\begin{aligned} \mathcal{Q}_{y_1^s} &= 57q, & \mathcal{Q}_{y_2^s} &= -18q, & \mathcal{Q}_{y_3^s} &= -17q & ; & \text{NO} \\ \mathcal{Q}_{y_1^s} &= \mp 17q, & \mathcal{Q}_{y_2^s} &= \pm 17q, & \mathcal{Q}_{y_3^s} &= 22q & ; & \text{IO} \end{aligned} \quad (52)$$

The hat Yukawa couplings $\hat{y}_{e,\mu,\tau}$ are fixed by the numerical values in Eq. (33) used in quark sector via the empirical ratios $m_e/m_\mu \doteq 4.84 \times 10^{-3}$, $m_\mu/m_\tau \doteq 5.95 \times 10^{-2}$, and $m_\tau/m_b \doteq 0.43$ in [26] as

$$\hat{y}_e = 0.713, \quad \hat{y}_\mu = 0.818, \quad \hat{y}_\tau = 0.431. \quad (53)$$

Through the $U(1)_X$ quantum numbers of Yukawa couplings of pseudo-Dirac neutrino sector, $\mathcal{Q}_{y_i^s}$ ($i = 1, 2, 3$), as shown in Eqs. (48), (50) and (52), the active neutrino mass spectra can be determined in terms of the new expansion parameters in Eq. (25) defined in quark sector; for example, in *case-I*, for NO ($\mathcal{Q}_{y_1^s} = 63q$, $\mathcal{Q}_{y_2^s} = -18q$, $\mathcal{Q}_{y_3^s} = -17q$):

$$\begin{aligned} m_{\nu_1} &\simeq \hat{y}_1^s \lambda^{\frac{189}{4}} \left| \frac{X_1 \delta_2^G}{X_2 \delta_1^G} \right|^{\frac{63}{2}} \left(\frac{B(1+\kappa^2)}{6\kappa^2} \frac{|\hat{y}_b|}{|\hat{Y}_d|} \right)^{\frac{63}{4}} v_u, \\ m_{\nu_2} &\simeq \hat{y}_2^s \lambda^{\frac{27}{2}} \left| \frac{X_1 \delta_2^G}{X_2 \delta_1^G} \right|^9 \left(\frac{B(1+\kappa^2)}{6\kappa^2} \frac{|\hat{y}_b|}{|\hat{Y}_d|} \right)^{\frac{9}{2}} v_u, \\ m_{\nu_3} &\simeq \hat{y}_3^s \lambda^{\frac{51}{4}} \left| \frac{X_1 \delta_2^G}{X_2 \delta_1^G} \right|^{\frac{17}{2}} \left(\frac{B(1+\kappa^2)}{6\kappa^2} \frac{|\hat{y}_b|}{|\hat{Y}_d|} \right)^{\frac{17}{4}} v_u, \end{aligned} \quad (54)$$

and, with the value ∇_Ψ in Eq. (33) obtained in quark sector the neutrino parameters are fixed within the 3σ constraints of the low energy neutrino oscillations [35] as

$$\hat{y}_2^s \ni (1.67, 1.79), \quad \hat{y}_3^s \ni (1.73, 1.82) \quad \hat{y}_1^s = \mathcal{O}(1); \quad (55)$$

for IO ($\mathcal{Q}_{y_1^s} = \mp 17q$, $\mathcal{Q}_{y_2^s} = \pm 17q$, $\mathcal{Q}_{y_3^s} = 28q$):

$$\begin{aligned} m_{\nu_1} &\simeq \hat{y}_1^s \lambda^{\frac{51}{4}} \left| \frac{X_1 \delta_2^G}{X_2 \delta_1^G} \right|^{\frac{17}{2}} \left(\frac{B(1+\kappa^2)}{6\kappa^2} \frac{|\hat{y}_b|}{|\hat{Y}_d|} \right)^{\frac{17}{4}} v_u, \\ m_{\nu_2} &\simeq \hat{y}_2^s \lambda^{\frac{51}{4}} \left| \frac{X_1 \delta_2^G}{X_2 \delta_1^G} \right|^{\frac{17}{2}} \left(\frac{B(1+\kappa^2)}{6\kappa^2} \frac{|\hat{y}_b|}{|\hat{Y}_d|} \right)^{\frac{17}{4}} v_u, \\ m_{\nu_3} &\simeq \hat{y}_3^s \lambda^{21} \left| \frac{X_1 \delta_2^G}{X_2 \delta_1^G} \right|^{14} \left(\frac{B(1+\kappa^2)}{6\kappa^2} \frac{|\hat{y}_b|}{|\hat{Y}_d|} \right)^7 v_u. \end{aligned} \quad (56)$$

and within the 3σ constraints of the low energy neutrino oscillations [35] by using the value ∇_Ψ in Eq. (33)

$$\hat{y}_{1,2}^s \ni (1.70, 1.81), \quad \hat{y}_3^s = \mathcal{O}(1). \quad (57)$$

However, there still remain two physical parameters undetermined, the scale of $U(1)_X$ symmetry breakdown and $\mathcal{Q}_{y_i^\nu}$, which correspond to the physical observables, the QCD axion mass and mass splittings Δm_k^2 for new neutrino oscillations through astronomical-scale baseline. Note that the neutrino mixing angles can be determined through the lepton Yukawa superpotential in Eq.(45) structured by the $SL_2(F_3)$ symmetry together with the desired VEV directions in Eqs. (11, 13, 15), as will be seen later.

A. Scale of PQ phase transition induced by Lepton sector

Now we are going to try to fix the scale of $U(1)_X$ symmetry breakdown, together with the constraints coming from the previous quark sector, by taking flavored-axion A_2 coupling to electron coming from the axion cooling of stars into account. Once the scale $f_{a2} = |X_2|\sqrt{2}v_\Psi$ is constrained by the constraints coming from rare flavor violating decay processes induced by flavored axions and axion cooling of stars, the scale $f_{a1} = |X_1|\sqrt{1+\kappa^2}v_\Theta$ associated to the seesaw scale could automatically be determined through Eq. (3).

As seen in superpotential (45) since the SM charged-lepton fields (which are nontrivially X -charged Dirac fermions) have $U(1)_{\text{EM}}$ charges, the axion A_2 coupling to electrons are added to the Lagrangian through a chiral rotation. And the axion A_2 couples directly to electrons, thereby the axion can be emitted by Compton scattering, atomic axio-recombination and axio-deexcitation, and axio-bremsstrahlung in electron-ion or electron-electron collisions [38]. The axion A_2 coupling to electron in the model reads

$$g_{Aee} = \frac{|X_e|m_e}{f_{a2}}, \quad \text{with } |X_e| = 6 \quad (58)$$

where $m_e = 0.511$ MeV. Such weakly coupled flavored-axion A_2 has a wealth of interesting phenomenological implications in the context of astrophysics¹⁹, like the formation of a cosmic diffuse background of axions from core collapse supernova explosions [36] or neutron star

¹⁹ From the cooling of white-dwarfs with the fine-structure of axion to electron, which is recently improved $4.1 \times 10^{-28} \lesssim \alpha_{Aee} \lesssim 3.7 \times 10^{-27}$ in Ref. [17], implying axion decay constant $f_{a2} = (1.42 - 4.27) \times 10^{10}$ GeV and its corresponding QCD axion decay constant $F_A = (0.34 - 1.01) \times 10^{10}$ GeV. See also the most recent analysis $\alpha_{Aee} = 2.04_{-0.77}^{+0.81} \times 10^{-27}$ at 1σ [19] leading to $f_{a2} = 1.92_{-0.29}^{+0.52} \times 10^{10}$ GeV which is interpreted as $F_A = 4.52_{-0.69}^{+1.22} \times 10^9$ GeV. These hints including Ref. [20] seem incompatible with the bound in Eq. (42) from the decay process $K^+ \rightarrow \pi + A_i$. However, if one relinquishes $N_{\text{DW}} = 1$ by considering $N_{\text{DW}} > 1$ in the case that the PQ phase transition happened during (or before) inflation, one can easily construct a model for accommodating the debating constraints under the present flavored-PQ scenario.

cooling [37]. There are several restrictive astrophysical limits [26] on the axion models that couples to electrons, which arise from the above mentioned processes: among them, (i) from stars in the red giant branch of the color-magnitude diagram of globular clusters [38], $\alpha_{Aee} < 1.5 \times 10^{-26}$ (95% CL) [39], (ii) from white dwarfs (WDs) where bremsstrahlung is mainly efficient [40], $\alpha_{Aee} < 6 \times 10^{-27}$ [17], (iii) from the Sun the XENON100 experiment provides the upper bound, $g_{Aee} < 7.7 \times 10^{-12}$ (90% CL) [41], and recently (iv) from the solar flux the PandaX-II experiment provides the upper bound $g_{Aee} < 4.35 \times 10^{-12}$ (90% CL) [42]. Here the fine-structure constant, $\alpha_{Aee} = g_{Aee}^2/4\pi$, is related to the axion-electron coupling constant g_{Aee} . Then, the astrophysical lower bound of the PQ breaking scale f_{a_2} and its corresponding QCD axion decay constant F_A is derived from the above mentioned upper limits

$$f_{a_2} > (3.98 \times 10^8 - 1.23 \times 10^{10}) \text{ GeV} \Leftrightarrow F_A > (9.38 \times 10^7 - 2.90 \times 10^9) \text{ GeV}. \quad (59)$$

Since this limit for the QCD axion decay constant is much lower than the bound from $K^+ \rightarrow \pi^+ + A_i$ in Eq. (43), we could not fix the scale of PQ phase transition. Nevertheless, assuming that in the near future the NA62 experiment [13] probes the flavored-axions, from the present upper bound in Eq. (43) and the future expected sensitivity of $\text{Br}(K^+ \rightarrow \pi^+ + A_i)$ in Eq. (44) we can take the central value:

$$F_A = 1.29 \times 10^{11} \text{ GeV}. \quad (60)$$

Hence, as shown in the left plot in FIG. 1, the model for $F_A = 1.29 \times 10^{11} \text{ GeV}$ expected from the future sensitivity of $\text{Br}(K^+ \rightarrow \pi^+ + A_i)$ has predictions (horizontal solid-red, dashed-blue, and dotted-black lines crossed by solid-red (case-I), dotted-blue (case-II), and dashed-black (case-III) lines, respectively) on the QCD axion mass m_a in terms of the Weinberg value $z = 0.56$, and the pion decay constant $f_\pi = 92 \text{ MeV}$ and $\mu m_u = (108.3 \text{ MeV})^2 z$,

$$m_a = \frac{f_\pi}{F_A} \left(\frac{\mu m_u}{1 + z + w} \right)^{\frac{1}{2}} = 45.8 \mu\text{eV}; \quad (61)$$

its axion photon coupling expressed in terms of the axion mass, pion mass, pion decay

constant, z and w ,

$$\begin{aligned}
|g_{a\gamma\gamma}| &= \frac{\alpha_{\text{em}}}{2\pi} \frac{m_a}{f_\pi m_{\pi^0}} \frac{1}{\sqrt{F(z, w)}} \left| \frac{E}{N} - \frac{2}{3} \frac{4 + z + w}{1 + z + w} \right| \\
&= \begin{cases} 1.72 \times 10^{-14} \text{ GeV}^{-1}; & \text{case-I : } (E/N = +23/6) \\ 1.12 \times 10^{-14} \text{ GeV}^{-1}; & \text{case-II : } (E/N = +19/6) \\ 8.37 \times 10^{-16} \text{ GeV}^{-1}; & \text{case-III : } (E/N = +11/6) \end{cases}. \quad (62)
\end{aligned}$$

The axion coupling to photon $g_{a\gamma\gamma}$ divided by the axion mass m_a is dependent on E/N . Left plot in Fig.1 shows the E/N dependence of $(g_{a\gamma\gamma}/m_a)^2$ so that the experimental limit is independent of the axion mass m_a [8]: the values of $(g_{a\gamma\gamma}/m_a)^2$ of our model are located lower than that of the experimentally excluded bound $(g_{a\gamma\gamma}/m_a)^2 \leq 1.44 \times 10^{-19} \text{ GeV}^{-2} \text{ eV}^{-2}$ from ADMX [43]. For the Weinberg value $z = 0.56$, the solid-red, dashed-blue, and dotted-black lines stand for $(g_{a\gamma\gamma}/m_a)^2 = 1.406 \times 10^{-19} \text{ GeV}^{-2} \text{ eV}^{-2}$ for the anomaly value $E/N = 23/6$ (case-I), $5.950 \times 10^{-20} \text{ GeV}^{-2} \text{ eV}^{-2}$ for $E/N = 19/6$ (case-II), and $3.342 \times 10^{-22} \text{ GeV}^{-2} \text{ eV}^{-2}$ for $E/N = 11/6$ (case-III), respectively.

B. Neutrinos

Even in the present model the quantum numbers $Q_{y_i^\nu}$ (or equivalently $Q_{L_{e,\mu,\tau}}$) are not uniquely determined through the model setup, together with the conditions above Eq. (46) their quantum numbers can be assigned by their corresponding physical observables which are the pseudo-Dirac mass splittings Δm_k^2 responsible for new oscillations available on high-energy neutrinos through astronomical-scale baseline [2, 45, 46].

As an explicit example, we take *case-I* in Eqs. (D5) and (47), and sequentially choose $y_i^\nu = \hat{y}_i^\nu \nabla_\Psi^9$ as

$$\begin{aligned}
-Q_{y_1^\nu} &= Q_{y_2^\nu} = Q_{y_3^\nu} = 9q & \text{for NO} \\
Q_{y_1^\nu} &= -Q_{y_2^\nu} = Q_{y_3^\nu} = -9q & \text{for IO}
\end{aligned} \quad , \quad (63)$$

by considering the conditions above Eq. (46). At energies below the electroweak scale, all leptons obtain masses. For the *case-I* the relevant lepton interaction terms with chiral

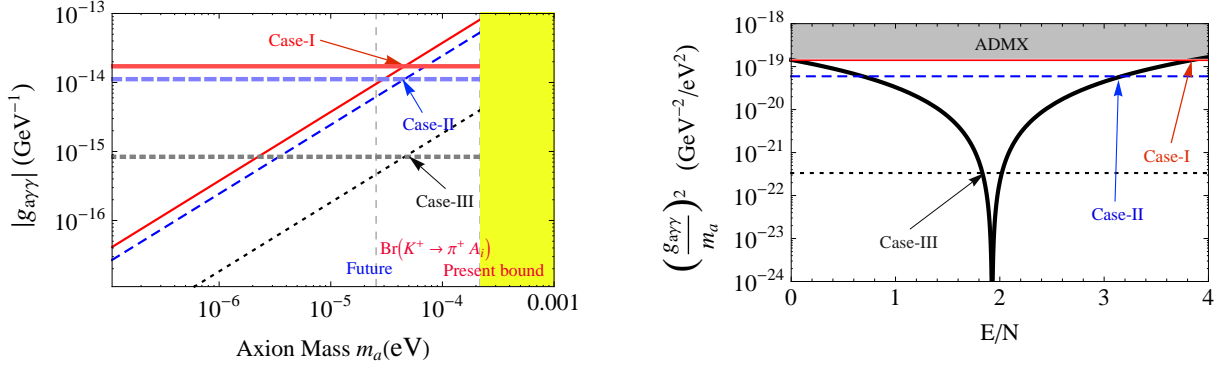


FIG. 1: Left plot for axion photon coupling $|g_{a\gamma\gamma}|$ as a function of the QCD axion mass m_a . Horizontal solid-red, dashed-blue, and dotted-black lines crossed by solid-red (case-I), dotted-blue (case-II), and dashed-black (case-III) lines show the model predictions for $F_A = 1.29 \times 10^{11}$ GeV expected from the future sensitivity of $\text{Br}(K^+ \rightarrow \pi^+ A_i)$: $|g_{a\gamma\gamma}| = 1.72 \times 10^{-14} \text{ GeV}^{-1}$, $1.12 \times 10^{-14} \text{ GeV}^{-1}$, and $8.37 \times 10^{-16} \text{ GeV}^{-1}$, respectively, with $m_a = 45.8 \mu\text{eV}$. The yellow-band indicates the excluded region derived from the present bound on $\text{Br}(K^+ \rightarrow \pi^+ A_i) < 7.3 \times 10^{-11}$ [16] (equivalently $m_a < 217 \mu\text{eV}$), while the vertical black-dashed line stands for the NA62 experiment future expected sensitivity of $\text{Br}(K^+ \rightarrow \pi^+ A_i) < 1.0 \times 10^{-12}$ [13] (equivalently $m_a < 25.5 \mu\text{eV}$). Right plot of $(g_{a\gamma\gamma}/m_a)^2$ versus E/N for $z = 0.56$. The gray-band represents the experimentally excluded bound $(g_{a\gamma\gamma}/m_a)^2 \leq 1.44 \times 10^{-19} \text{ GeV}^{-2} \text{ eV}^{-2}$ from ADMX [43]. Here the solid-red, dashed-blue, and dotted-black lines stand for $(g_{a\gamma\gamma}/m_a)^2 = 1.406 \times 10^{-19} \text{ GeV}^{-2} \text{ eV}^{-2}$ for $E/N = 23/6$ (case-I), $5.950 \times 10^{-20} \text{ GeV}^{-2} \text{ eV}^{-2}$ for $E/N = 19/6$ (case-II), and $3.342 \times 10^{-22} \text{ GeV}^{-2} \text{ eV}^{-2}$ for $E/N = 11/6$ (case-III), respectively. See more various supersymmetric and non-supersymmetric type models varying the parameter E/N in Refs. [2, 44].

fermions is given by

$$\begin{aligned}
-\mathcal{L}_Y^{\ell\nu} = & \bar{\ell}_R \mathcal{M}_\ell \ell_L + \frac{g}{\sqrt{2}} W_\mu^- \bar{\ell}_L \gamma^\mu \nu_L \\
& + \frac{1}{2} \begin{pmatrix} \bar{\nu}_L^c & \bar{S}_R & \bar{N}_R \end{pmatrix} \begin{pmatrix} 0 & m_{DS}^T & m_D^T \\ m_{DS} & e^{i\frac{A_1}{v_F}} M_S & 0 \\ m_D & 0 & e^{i\frac{A_1}{v_F}} M_R \end{pmatrix} \begin{pmatrix} \nu_L \\ S_R^c \\ N_R^c \end{pmatrix} + \text{h.c.} \quad (64)
\end{aligned}$$

And in the above Lagrangian (64) the charged-lepton and heavy Majorana neutrino mass

terms read

$$\mathcal{M}_\ell = \begin{pmatrix} \hat{y}_e \nabla_\Psi^6 e^{6i\frac{A_2}{v_g}} & 0 & 0 \\ 0 & \hat{y}_\mu \nabla_\Psi^3 e^{-3i\frac{A_2}{v_g}} & 0 \\ 0 & 0 & \hat{y}_\tau \nabla_\Psi e^{i\frac{A_2}{v_g}} \end{pmatrix} v_d, \quad (65)$$

$$M_R = \begin{pmatrix} 1 + \frac{2}{3}\tilde{\kappa} e^{i\phi} & -\frac{1}{3}\tilde{\kappa} e^{i\phi} & -\frac{1}{3}\tilde{\kappa} e^{i\phi} \\ -\frac{1}{3}\tilde{\kappa} e^{i\phi} & \frac{2}{3}\tilde{\kappa} e^{i\phi} & 1 - \frac{1}{3}\tilde{\kappa} e^{i\phi} \\ -\frac{1}{3}\tilde{\kappa} e^{i\phi} & 1 - \frac{1}{3}\tilde{\kappa} e^{i\phi} & \frac{2}{3}\tilde{\kappa} e^{i\phi} \end{pmatrix} M, \quad (66)$$

where

$$\tilde{\kappa} \equiv \kappa \left| \frac{\hat{y}_R}{\hat{y}_\Theta} \right|, \quad \phi \equiv \arg \left(\frac{\hat{y}_R}{\hat{y}_\Theta} \right) \quad \text{with} \quad M \equiv \left| \hat{y}_\Theta \frac{v_\Theta}{\sqrt{2}} \right|. \quad (67)$$

For NO, the Dirac and Majorana mass terms read

$$m_{DS} = \begin{pmatrix} \hat{y}_1^s \nabla_\Psi^{63} e^{-63i\frac{A_2}{v_g}} & 0 & 0 \\ 0 & \hat{y}_2^s \nabla_\Psi^{18} e^{18i\frac{A_2}{v_g}} & 0 \\ 0 & 0 & \hat{y}_3^s \nabla_\Psi^{17} e^{17i\frac{A_2}{v_g}} \end{pmatrix} v_u, \quad (68)$$

$$M_S = \begin{pmatrix} \hat{y}_1^{ss} \nabla_\Psi^{144} e^{-144i\frac{A_2}{v_g}} & 0 & 0 \\ 0 & 0 & \hat{y}_2^{ss} \nabla_\Psi^{54} e^{54i\frac{A_2}{v_g}} \\ 0 & \hat{y}_2^{ss} \nabla_\Psi^{54} e^{54i\frac{A_2}{v_g}} & 0 \end{pmatrix} \nabla_\Theta \frac{v_\Theta}{\sqrt{2}}, \quad (69)$$

$$m_D = \hat{y}_1^\nu \begin{pmatrix} e^{9i\frac{A_2}{v_g}} & 0 & 0 \\ 0 & 0 & y_2 e^{-9i\frac{A_2}{v_g}} \\ 0 & y_3 e^{-9i\frac{A_2}{v_g}} & 0 \end{pmatrix} \nabla_T \nabla_\Psi^9 v_u, \quad (70)$$

where $y_2 \equiv \hat{y}_2^\nu / \hat{y}_1^\nu$ and $y_3 \equiv \hat{y}_3^\nu / \hat{y}_1^\nu$. For IO, the Dirac and Majorana mass terms read

$$m_{DS} = \begin{pmatrix} \hat{y}_1^s \nabla_\Psi^{17} e^{-17i\frac{A_2}{v_g}} & 0 & 0 \\ 0 & \hat{y}_2^s \nabla_\Psi^{17} e^{17i\frac{A_2}{v_g}} & 0 \\ 0 & 0 & \hat{y}_3^s \nabla_\Psi^{28} e^{-28i\frac{A_2}{v_g}} \end{pmatrix} v_u, \quad (71)$$

$$M_S = \begin{pmatrix} \hat{y}_1^{ss} \nabla_\Psi^{52} e^{-52i\frac{A_2}{v_g}} & 0 & 0 \\ 0 & 0 & \hat{y}_2^{ss} \nabla_\Psi^{29} e^{-29i\frac{A_2}{v_g}} \\ 0 & \hat{y}_2^{ss} \nabla_\Psi^{29} e^{-29i\frac{A_2}{v_g}} & 0 \end{pmatrix} \nabla_\Theta \frac{v_\Theta}{\sqrt{2}}, \quad (72)$$

$$m_D = \hat{y}_1^\nu \begin{pmatrix} e^{9i\frac{A_2}{v_g}} & 0 & 0 \\ 0 & 0 & y_2 e^{-9i\frac{A_2}{v_g}} \\ 0 & y_3 e^{9i\frac{A_2}{v_g}} & 0 \end{pmatrix} \nabla_T \nabla_\Psi^9 v_u. \quad (73)$$

Reminding that the hat Yukawa couplings in Eqs. (66-73) are all of order unity and complex numbers. From Eq. (64), by redefining the light neutrino field ν_L as $P_\nu \nu_L$ and transforming $\ell_L \rightarrow P_\nu \ell_L$, $\ell_R \rightarrow P_\nu \ell_R$, $S_R \rightarrow P_s S_R$ where $P_{\nu,s}$ are diagonalized matrices of arbitrary phases, one can always make the Dirac neutrino Yukawa couplings \hat{y}_1^ν , y_2 , y_3 and \hat{y}_1^s , \hat{y}_2^s , \hat{y}_3^s real and positive; then the parameters $\tilde{\kappa}$ and $y_{2,3}$ lie in the real and positive ranges

$$0.17 \lesssim \tilde{\kappa} \lesssim 16.63, \quad 0.1 \lesssim y_{2,3} \lesssim 10, \quad (74)$$

which will be used in numerical analysis, later.

After seesawing [2] due to the scale in Eq. (60) (or see Eqs. (43) and (59)) much larger than the electroweak scale, in a basis where charged lepton and heavy neutrino masses are real and diagonal, we obtain an effective light neutrino mass matrix in the basis (ν_L, S_R^c)

$$\mathcal{M}_\nu = \begin{pmatrix} \delta_\nu & m_\nu^T \\ m_\nu & M_S \end{pmatrix}. \quad (75)$$

Under the given quantum numbers the active neutrinos appear as pseudo-Dirac neutrinos. And the pseudo-Dirac mass splittings in k -th pair $\Delta m_k^2 \equiv m_{\nu_k}^2 - m_{S_k}^2$ are expressed as

$$\Delta m_k^2 = 2 m_k |\delta_k^\nu| \ll m_{\nu_k} \quad (76)$$

for all $k = 1, 2, 3$, where m_{ν_k} and m_{S_k} are mass eigenvalues of the effective mass matrix in Eq. (75) and δ_k^ν are mass eigenvalues of the seesaw formula $\delta_\nu = -m_D^T M_R^{-1} m_D$. Eq. (76) shows that both the active neutrino masses m_{ν_k} coming from the matrix $m_\nu \equiv m_{DS}$ in Eq. (68) and the PMNS leptonic mixing angles coming from the matrix δ_ν are closely tied to Δm_k^2 responsible for long wavelengths. Here the active neutrino masses we consider are given in Eq. (54) for NO and Eq (56) for IO. On the other hand, the neutrino mixing parameters are determined by

$$\begin{aligned} \delta_\nu &= -m_D^T M_R^{-1} m_D = m_0 \begin{pmatrix} 1 + 2F & (1 - F)y_2 & (1 - F)y_3 \\ (1 - F)y_2 & (1 + \frac{F-3G}{2})y_2^2 & (1 + \frac{F+3G}{2})y_2 y_3 \\ (1 - F)y_3 & (1 + \frac{F+3G}{2})y_2 y_3 & (1 + \frac{F-3G}{2})y_3^2 \end{pmatrix} \\ &= U_{\text{PMNS}}^* \text{diag}(\delta_1^\nu, \delta_2^\nu, \delta_3^\nu) U_{\text{PMNS}}^\dagger, \end{aligned} \quad (77)$$

where the leptonic PMNS matrix U_{PMNS} [26] is given by Eq. (C1), and

$$F = (\tilde{\kappa} e^{i\phi} + 1)^{-1}, \quad G = (\tilde{\kappa} e^{i\phi} - 1)^{-1}, \quad m_0 = \left| \frac{\hat{y}_1^{\nu^2} v_u^2}{3M} \right| \nabla_T^2 \nabla_\Psi^{18}. \quad (78)$$

In the limit of $y_2, y_3 \rightarrow 1$ the above mass matrix reflects exact TBM mixing [47] and its corresponding mass eigenvalues $|\delta_1^\nu| = 3m_0|F|$, $|\delta_2^\nu| = 3m_0$, $|\delta_3^\nu| = 3m_0|G|$. Since in general it is expected deviations of $y_{2,3}$ from unity, Eq. (77) directly indicates that there could be deviations from the exact TBM, leading to a possibility to search for CP violation in neutrino oscillation experiments. In addition, due to the small value of θ_{13} it is expected $|\delta_1^\nu| \simeq |\delta_2^\nu| \simeq |\delta_3^\nu| \approx 3m_0$. To obtain the pseudo-Dirac mass splittings, taking the scale of heavy neutrino $M = \hat{y}_\Theta f_{a_1}/(|X_1|\sqrt{2(1+\kappa^2)})$ in Eq. (67)

$$M \simeq 2 \times 10^{11} \text{ GeV} \quad (79)$$

from the QCD axion decay constant in Eq. (60) and using the best-fit values of the low energy neutrino oscillations [35], we can obtain the pseudo-Dirac mass splittings in a good approximation:

$$\Delta m_3^2 \simeq 4.1 \times 10^{-14} \text{ eV}^2, \quad \Delta m_2^2 \simeq 7.1 \times 10^{-15} \text{ eV}^2, \quad \Delta m_1^2 \simeq 3.5 \times 10^{-36} \text{ eV}^2, \quad (80)$$

for NO with $\hat{y}_1^s = 1$;

$$\Delta m_2^2 \simeq 4.1 \times 10^{-14} \text{ eV}^2 \simeq \Delta m_1^2, \quad \Delta m_3^2 \simeq 2.5 \times 10^{-22} \text{ eV}^2, \quad (81)$$

for IO with $\hat{y}_3^s = 1$.

Due to the precise measurement of θ_{13} , which is relatively large, it may now be possible to put constraints on the Dirac phase δ_{CP} which will be obtained in the long baseline neutrino oscillation experiments T2K [48], NO ν A [49], MINOS [50] etc.. However, the current large uncertainty on θ_{23} is at present limiting the information that can be extracted from the ν_e appearance measurements. Precise measurements of all the mixing angles, especially θ_{23} , are needed to maximize the sensitivity to the leptonic CP violation. The active neutrino oscillation experiments are now on a new step to confirm the CP violation and octant of atmospheric mixing angle θ_{23} in the lepton sector. Actually, the recent data of T2K and NO ν A experiments indicate a finite CP phase [51] together with their preferred octant on θ_{23} [48, 49].

C. Numerical analysis for neutrino mixing parameters

In order to show model predictions on the leptonic Dirac CP phase δ_{CP} incident to the atmospheric mixing angle θ_{23} , we perform a numerical simulation by using the linear algebra tools of Ref. [29] with the 3σ constraints of the low energy neutrino oscillations [35].

In our numerical analysis, we take²⁰ $M = 2 \times 10^{11}$ GeV in Eq. (79) and $\tan\beta = 7.40$ (see Eq. (60) and Eq. (32)), as inputs. The seesaw formula in Eq. (77) for obtaining neutrino mixing parameters ($\theta_{12}, \theta_{13}, \theta_{23}, \delta_{CP}$) and their eigenvalues $\delta_k^\nu = \Delta m_k^2 / 2m_{\nu_k}$ ($k = 1, 2, 3$) contains seven parameters: $y_1 (\equiv \hat{y}_1^\nu \nabla_T \nabla_\Psi^9), v_u, M, y_2, y_3, \tilde{\kappa}, \phi$. The first three (y_1, M , and v_u) lead to the overall scale parameter m_0 in Eq. (78), which is closely related to the $U(1)_{X_1}$ breaking scale. The next four ($y_2, y_3, \tilde{\kappa}, \phi$) with the allowed ranges in Eq. (74) give rise to the deviations from TBM, the CP phases, and corrections to the pseudo-Dirac mass splittings $\Delta m_k^2 = 2m_k |\delta_k|$. Since the individual neutrino masses ($m_{\nu_k} = m_k$) are determined as in Eqs. (54) and (56) within the 3σ constraints of the low energy neutrino oscillations [35], for numerical simulation we can simply fix the pseudo-Dirac mass splittings²¹ $\Delta m_k^2 = 2m_k |\delta_k|$, without loss of generality, as in Eq. (80) for NO and Eq. (81) for IO. Then, the active neutrino masses m_{ν_k} can directly be linked to the eigenvalues δ_k^ν in Eq. (77).

Hence, there are only left the five physical parameters $m_0, y_2, y_3, \tilde{\kappa}, \phi$ contained in Eq. (77), which can be determined from the 3σ experimental bounds of three mixing angles ($\theta_{12}, \theta_{13}, \theta_{23}$) and two active neutrino mass splittings ($\Delta m_{\text{Sol}}^2, \Delta m_{\text{Atm}}^2$). Among nine observables (six mixing parameters $\theta_{12}, \theta_{23}, \theta_{13}, \delta_{CP}, \varphi_{1,2}$ and three mass eigenvalues $m_{\nu_1}, m_{\nu_2}, m_{\nu_3}$) in low energy neutrino sector, the remaining four observables (one Dirac CP phase δ_{CP} , two Majorana CP phases $\varphi_{1,2}$, and one active neutrino mass) can be predicted in the model. Here both the lightest active neutrino mass and the Majorana CP phases contributing to the effective active neutrino masses are negligibly small enough in the model. Therefore, we can have reasonable model predictions on the Dirac CP phase δ_{CP} incident to behavior of the large uncertainty on θ_{23} .

The recent analysis based on global fits [35, 53, 54] of the neutrino oscillations enters into a new phase of precise determination of mixing angles and mass squared differences: we take the global fits at 3σ [35], shown in Table IV, as experimental constraints.

Scanning all the parameter spaces ($0.17 \lesssim \tilde{\kappa} \lesssim 16.63$, $0.1 \lesssim y_{2,3} \lesssim 10$ in Eq. (74), $1/\sqrt{10} \lesssim \hat{y}_1^\nu \lesssim \sqrt{10}$, and $0 \leq \phi \leq 2\pi$) by putting the experimental 3σ constraints in Table IV with the above input parameters:

For NO with the setting of pseudo-Dirac mass splittings $\Delta m_3^2 = 4.1 \times 10^{-14} \text{ eV}^2$, $\Delta m_2^2 =$

²⁰ From Eqs. (60) and (67) we reasonably well square the axion decay constant f_{a_1} with the scale M .

²¹ They may be fixed by high energy astronomical-baseline experiments, such as IceCube [52].

TABLE IV: The global fit of three-flavor oscillation parameters at 3σ level [35]. NO = normal neutrino mass ordering; IO = inverted mass ordering. And $\Delta m_{\text{Sol}}^2 \equiv m_{\nu_2}^2 - m_{\nu_1}^2$, $\Delta m_{\text{Atm}}^2 \equiv m_{\nu_3}^2 - m_{\nu_1}^2$ for NO, and $\Delta m_{\text{Atm}}^2 \equiv m_{\nu_2}^2 - m_{\nu_3}^2$ for IO.

	$\theta_{13}[^{\circ}]$	$\delta_{CP}[^{\circ}]$	$\theta_{12}[^{\circ}]$	$\theta_{23}[^{\circ}]$	$\Delta m_{\text{Sol}}^2 [10^{-5} \text{eV}^2]$	$\Delta m_{\text{Atm}}^2 [10^{-3} \text{eV}^2]$
3σ NO	$7.99 \rightarrow 8.90$	$0 \rightarrow 360$	$31.38 \rightarrow 35.99$	$38.4 \rightarrow 52.8$	$7.03 \rightarrow 8.09$	$2.407 \rightarrow 2.643$
IO	$8.03 \rightarrow 8.93$			$38.8 \rightarrow 53.1$		$2.399 \rightarrow 2.635$

$7.1 \times 10^{-15} \text{eV}^2$, $\Delta m_1^2 = 3.5 \times 10^{-36} \text{eV}^2$ in Eq. (80) the neutrino parameter spaces are fixed as

$$\begin{aligned} \tilde{\kappa} &\in [0.17, 0.36], & \phi &\in [91^{\circ}, 95^{\circ}] \cup [265^{\circ}, 270^{\circ}], \\ \hat{y}_1^{\nu} &\in [1.06, 1.15], & y_2 &\in [0.87, 1.12], & y_3 &\in [0.89, 1.12], \end{aligned} \quad (82)$$

for $\Delta m_2^2/\Delta m_3^2 \geq m_{\nu_2}/m_{\nu_3}$ (or equivalently $\delta_2^{\nu}/\delta_3^{\nu} \geq 1$), indicating red-asters in the left plot of FIG. 2;

$$\begin{aligned} \tilde{\kappa} &\in [0.17, 0.30], & \phi &\in [85^{\circ}, 100^{\circ}] \cup [265^{\circ}, 274^{\circ}], \\ \hat{y}_1^{\nu} &\in [1.06, 1.10], & y_2 &\in [0.93, 1.12], & y_3 &\in [0.22, 1.12], \end{aligned} \quad (83)$$

for $\Delta m_2^2/\Delta m_3^2 < m_{\nu_2}/m_{\nu_3}$ (or equivalently $\delta_2^{\nu}/\delta_3^{\nu} < 1$), indicating blue-spots in the left plot of FIG. 2.

For IO with the setting of pseudo-Dirac mass splittings $\Delta m_2^2 = 4.1 \times 10^{-14} \text{eV}^2 = \Delta m_1^2$, $\Delta m_3^2 = 2.5 \times 10^{-22} \text{eV}^2$ in Eq. (81) we obtain

$$\begin{aligned} \tilde{\kappa} &\in [0.17, 0.66], & \phi &\in [92^{\circ}, 110^{\circ}] \cup [260^{\circ}, 268^{\circ}], \\ \hat{y}_1^{\nu} &\in [1.06, 1.13], & y_2 &\in [0.80, 1.20], & y_3 &\in [0.81, 1.21]. \end{aligned} \quad (84)$$

As shown in FIG. 2 there are remarkable predictions on δ_{CP} as a function of the atmospheric mixing angle θ_{23} for NO (left plot) and IO (right plot). Moreover, in the model, the neutrinoless-double-beta ($0\nu\beta\beta$)-decay rate effectively measures the absolute value of the ee -component of the effective neutrino mass matrix \mathcal{M}_{ν} in Eq. (75) in the basis where the charged lepton mass matrix is real and diagonal, which can be expressed as $|m_{ee}| = |\sum_{k=1}^3 (U_{ek}/\sqrt{2})^2 (m_{\nu_k} - m_{S_k})|$. Thus, accurate measurements of θ_{23} and δ_{CP} are crucial for a test of our model. In addition, the discovery of $0\nu\beta\beta$ -decay in the on-going or

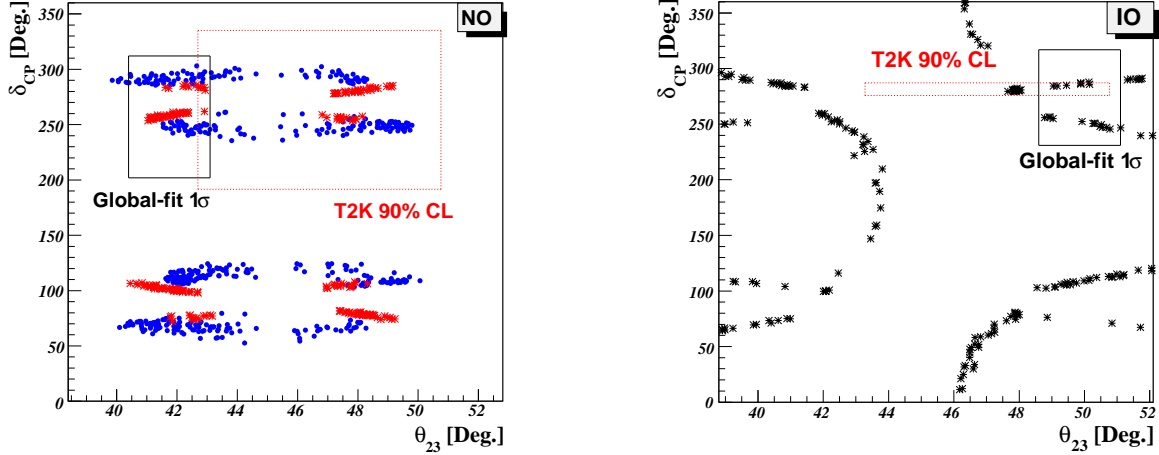


FIG. 2: Plot for leptonic Dirac CP phase δ_{CP} as a function of the atmospheric mixing angle θ_{23} . In the left plot for NO, red-asters indicate the case of $\Delta m_2^2/\Delta m_3^2 \geq \sqrt{\Delta m_{\text{Sol}}^2/\Delta m_{\text{Atm}}^2}$ and blue-spots for $\Delta m_2^2/\Delta m_3^2 < \sqrt{\Delta m_{\text{Sol}}^2/\Delta m_{\text{Atm}}^2}$. In the left plot, black-quadrangle represents global-fit 1σ bounds $\delta_{CP}/[^\circ] = 261_{-59}^{+51}$ and $\theta_{23}/[^\circ] = 41.6_{-1.2}^{+1.5}$ [35], while red-dotted quadrangle favored by T2K [56] stands for 90% CL bounds $\delta_{CP}/[^\circ] = [191.0, 334.8]$ and $\theta_{23}/[^\circ] = 47.9_{-5.2}^{+2.9}$. Right plot for IO, where black-quadrangle for global-fit 1σ bounds $\delta_{CP}/[^\circ] = 277_{-46}^{+40}$ and $\theta_{23}/[^\circ] = 50.0_{-1.4}^{+1.1}$ [35], while red-dotted quadrangle favored by T2K [56] for 90% CL bounds $\delta_{CP}/[^\circ] = [275.8, 287.2]$ and $\theta_{23}/[^\circ] = 47.9_{-4.6}^{+2.9}$.

future $0\nu\beta\beta$ -decay experiments [55], with sensitivities $0.01 < |m_{ee}|/\text{eV} < 0.1$, will rule out the present model.

In the left plot (NO) of FIG.2, with the sum of neutrino masses $\sum_{i=1}^3 m_{\nu_i} \ni [0.058, 0.060] \text{eV}$ and the amplitude of $0\nu\beta\beta$ -decay rate $|m_{ee}| \simeq 4 \times 10^{-13} \text{eV}$, the red-asters stand for predictions on

$$\begin{aligned} \theta_{23} &\ni [40.5^\circ, 43.2^\circ] \cup [48.8^\circ, 49.2^\circ], \\ \delta_{CP} &\ni [72.1^\circ, 81.7^\circ] \cup [98.0^\circ, 107.8^\circ] \cup [253.6^\circ, 262.0^\circ] \cup [278.0^\circ, 285.8^\circ], \end{aligned} \quad (85)$$

for $\Delta m_2^2/\Delta m_3^2 \geq m_{\nu_2}/m_{\nu_3}$; similarly, the blue-spots indicate predictions on

$$\begin{aligned} \theta_{23} &\ni [40.0^\circ, 44.2^\circ] \cup [45.4^\circ, 50.1^\circ], \\ \delta_{CP} &\ni [52.5^\circ, 79.5^\circ] \cup [103.3^\circ, 124.4^\circ] \cup [236.0^\circ, 257.4^\circ] \cup [285.4^\circ, 303.0^\circ], \end{aligned} \quad (86)$$

for $\Delta m_2^2/\Delta m_3^2 < m_{\nu_2}/m_{\nu_3}$. On the other hand, in the right plot (IO) of FIG.2 with the sum of neutrino masses $\sum_{i=1}^3 m_{\nu_i} \ni (0.097, 0.102) \text{eV}$ and the amplitude of $0\nu\beta\beta$ -decay rate

$|m_{ee}| \simeq 4 \times 10^{-13}$ eV, the black-crosses stand for predictions on

$$\delta_{CP} \ni [65.0^\circ, 295.5^\circ], \quad \text{for } \theta_{23} \ni [38.9^\circ, 43.8^\circ]; \quad (87)$$

$$\delta_{CP} \ni [11.3^\circ, 120.0^\circ] \cup [235.7^\circ, 360.0^\circ], \quad \text{for } \theta_{23} \ni [46.2^\circ, 52.8^\circ]. \quad (88)$$

Even the results for IO look like having wide ranges, as shown in the right plot (IO) of FIG. 2 there is a remarkable predictive-pattern for δ_{CP} as a function of θ_{23} .

VI. CONCLUSION

We have constructed a minimalistic SUSY model for quarks, leptons, and flavored-axions (and its one linear combination, QCD axion) through the argument that the $U(1)$ mixed-gravitational anomaly cancellation could be of central importance in constraining the fermion content of a new chiral gauge theory. It contains a flavor-structured $G_F = SL_2(F_3) \times U(1)_X$ symmetry for a compact description of new physics beyond SM. We have showed that axionic domain-wall condition N_{DW} with the $U(1)_X$ mixed-gravitational anomaly cancellation depends on both $U(1)_X$ charged quark and lepton flavors; the scale of PQ symmetry breakdown congruent to the seesaw scale is constrained through constraints coming from astrophysics and particle physics. Along this line, we have showed that the model could well be flavor-structured by the G_F symmetry in a unique way that domain-wall number $N_{\text{DW}} = 1$ with the $U(1)_X$ mixed-gravitational anomaly-free condition demands additional Majorana fermions as well as the flavor puzzles of SM are well delineated by new expansion parameters defined by the model dependent parameters, $U(1)_X$ charges and $U(1)_X$ - $[SU(3)_C]^2$ anomaly coefficients. In turn, we have showed that the flavored-axion model works well by performing a numerical simulation for the quark sector, leading to $\tan\beta = 7.40$ with the experimental results of the CKM mixing angles and their corresponding quark masses satisfied, as shown in Sec. IV A.

And we have showed that the constraint on the $U(1)_X$ symmetry breaking scale coming from the particle physics on the rare decay $K^+ \rightarrow \pi^+ + A_i$ is much stronger than that from the astroparticle physics on QCD axion and flavored-axion cooling of stars. So, in order to fix the scale of PQ phase transition we take a testable QCD axion decay constant, $F_A = 1.29 \times 10^{11}$ GeV, from the current bound and the future expected sensitivity on $\text{Br}(K^+ \rightarrow \pi^+ + A_i)$, which gives model predictions on the axion mass $m_a = 45.8 \mu\text{eV}$ and axion-photon couplings

$|g_{a\gamma\gamma}| = 1.72 \times 10^{-14} \text{ GeV}^{-1}$ for $E/N = +23/6$ (case-I), $1.12 \times 10^{-14} \text{ GeV}^{-1}$ for $E/N = +19/6$ (case-II), and $8.37 \times 10^{-16} \text{ GeV}^{-1}$ for $E/N = +11/6$ (case-III), as summarized in FIG. 1 for QCD axion.

Subsequently, we have showed that the lepton sector structured by the symmetry G_F provides interesting physical implications on neutrino: hierarchical mass spectra and unmeasurable neutrinoless-double-beta decay rate with the interesting predictions on atmospheric mixing angle and leptonic Dirac CP phase favored by the recent long-baseline neutrino oscillation experiments, as summarized in FIG. 2 for NO and IO.

Appendix A: The $SL_2(F_3)$ group

The $SL_2(F_3)$ is the double covering of the tetrahedral group A_4 [7, 9, 10]. It contains 24 elements and has three kinds of representations: one triplet $\mathbf{3}$ and three singlets $\mathbf{1}$, $\mathbf{1}'$ and $\mathbf{1}''$, and three doublets $\mathbf{2}$, $\mathbf{2}'$ and $\mathbf{2}''$. The representations $\mathbf{1}'$, $\mathbf{1}''$ and $\mathbf{2}'$, $\mathbf{2}''$ are complex conjugated to each other. Note that A_4 is not a subgroup of $SL_2(F_3)$, since the two-dimensional representations cannot be decomposed into representations of A_4 . The generators S and T satisfy the required conditions $S^2 = R$, $T^3 = 1$, $(ST)^3 = 1$, and $R^2 = 1$, where $R = 1$ in case of the odd-dimensional representation and $R = -1$ for $\mathbf{2}$, $\mathbf{2}'$ and $\mathbf{2}''$ such that R commutes with all elements of the group. The matrices S and T representing the generators depend on the representations of the group [10]:

$\mathbf{1}$	$S = 1$	$T = 1$
$\mathbf{1}'$	$S = 1$	$T = \omega$
$\mathbf{1}''$	$S = 1$	$T = \omega^2$
$\mathbf{2}$	$S = A_1$	$T = \omega A_2$
$\mathbf{2}'$	$S = A_1$	$T = \omega^2 A_2$
$\mathbf{2}''$	$S = A_1$	$T = A_2$
$\mathbf{3}$	$S = \frac{1}{3} \begin{pmatrix} -1 & 2\omega & 2\omega^2 \\ 2\omega^2 & -1 & 2\omega \\ 2\omega & 2\omega^2 & -1 \end{pmatrix}$	$T = \begin{pmatrix} 1 & 0 & 0 \\ 0 & \omega & 0 \\ 0 & 0 & \omega^2 \end{pmatrix}$

where we have used the matrices

$$A_1 = -\frac{1}{\sqrt{3}} \begin{pmatrix} i & \sqrt{2}e^{i\pi/12} \\ -\sqrt{2}e^{-i\pi/12} & -i \end{pmatrix} \quad A_2 = \begin{pmatrix} \omega & 0 \\ 0 & 1 \end{pmatrix}.$$

The following multiplication rules between the various representations are calculated in Ref. [10], where α_i indicate the elements of the first representation of the product and β_i indicate those of the second representation. Moreover $a, b = 0, \pm 1$ and we denote $1^0 \equiv 1$, $1^1 \equiv 1'$, $1^{-1} \equiv 1''$ and similarly for the doublet representations. On the right-hand side the sum $a + b$ is modulo 3.

The multiplication rules with the 1-dimensional representations are the following:

$$1 \otimes Rep = Rep \otimes 1 = Rep \quad \text{with } Rep \text{ whatever representation}$$

$$1^a \otimes 1^b = 1^b \otimes 1^a = 1^{a+b} \equiv \alpha\beta$$

$$1^a \otimes 2^b = 2^b \otimes 1^a = 2^{a+b} \equiv \begin{pmatrix} \alpha\beta_1, & \alpha\beta_2 \end{pmatrix}$$

$$1' \otimes 3 = 3 = \begin{pmatrix} \alpha\beta_3, & \alpha\beta_1, & \alpha\beta_2 \end{pmatrix}, \quad 1'' \otimes 3 = 3 = \begin{pmatrix} \alpha\beta_2, & \alpha\beta_3, & \alpha\beta_1 \end{pmatrix}.$$

The multiplication rules with the 2-dimensional representations are

$$2 \otimes 2 = 2' \otimes 2'' = 2'' \otimes 2' = 3 \oplus 1$$

$$\text{with} \quad 3 = \begin{pmatrix} \frac{1-i}{2}(\alpha_1\beta_2 + \alpha_2\beta_1), & i\alpha_1\beta_1, & \alpha_2\beta_2 \end{pmatrix}, \quad 1 = \alpha_1\beta_2 - \alpha_2\beta_1;$$

$$2 \otimes 2' = 2'' \otimes 2'' = 3 \oplus 1'$$

$$\text{with} \quad 3 = \begin{pmatrix} \alpha_2\beta_2, & \frac{1-i}{2}(\alpha_1\beta_2 + \alpha_2\beta_1), & i\alpha_1\beta_1 \end{pmatrix}, \quad 1' = \alpha_1\beta_2 - \alpha_2\beta_1;$$

$$2 \otimes 2'' = 2' \otimes 2' = 3 \oplus 1''$$

$$\text{with} \quad 3 = \begin{pmatrix} i\alpha_1\beta_1, & \alpha_2\beta_2, & \frac{1-i}{2}(\alpha_1\beta_2 + \alpha_2\beta_1) \end{pmatrix}, \quad 1'' = \alpha_1\beta_2 - \alpha_2\beta_1;$$

$$2 \otimes 3 = 2 \oplus 2' \oplus 2''$$

$$\text{with} \quad \begin{aligned} 2 &= \begin{pmatrix} (1+i)\alpha_2\beta_2 + \alpha_1\beta_1, & (1-i)\alpha_1\beta_3 - \alpha_2\beta_1 \end{pmatrix} \\ 2' &= \begin{pmatrix} (1+i)\alpha_2\beta_3 + \alpha_1\beta_2, & (1-i)\alpha_1\beta_1 - \alpha_2\beta_2 \end{pmatrix} \\ 2'' &= \begin{pmatrix} (1+i)\alpha_2\beta_1 + \alpha_1\beta_3, & (1-i)\alpha_1\beta_2 - \alpha_2\beta_3 \end{pmatrix}; \end{aligned}$$

$$2' \otimes 3 = 2 \oplus 2' \oplus 2''$$

$$\text{with} \quad \begin{aligned} 2 &= \begin{pmatrix} (1+i)\alpha_2\beta_1 + \alpha_1\beta_3, & (1-i)\alpha_1\beta_2 - \alpha_2\beta_3 \end{pmatrix} \\ 2' &= \begin{pmatrix} (1+i)\alpha_2\beta_2 + \alpha_1\beta_1, & (1-i)\alpha_1\beta_3 - \alpha_2\beta_1 \end{pmatrix} \\ 2'' &= \begin{pmatrix} (1+i)\alpha_2\beta_3 + \alpha_1\beta_2, & (1-i)\alpha_1\beta_1 - \alpha_2\beta_2 \end{pmatrix}; \end{aligned}$$

$$2'' \otimes 3 = 2 \oplus 2' \oplus 2''$$

$$\text{with} \quad \begin{aligned} 2 &= \begin{pmatrix} (1+i)\alpha_2\beta_3 + \alpha_1\beta_2, & (1-i)\alpha_1\beta_1 - \alpha_2\beta_2 \end{pmatrix} \\ 2' &= \begin{pmatrix} (1+i)\alpha_2\beta_1 + \alpha_1\beta_3, & (1-i)\alpha_1\beta_2 - \alpha_2\beta_3 \end{pmatrix} \\ 2'' &= \begin{pmatrix} (1+i)\alpha_2\beta_2 + \alpha_1\beta_1, & (1-i)\alpha_1\beta_3 - \alpha_2\beta_1 \end{pmatrix}. \end{aligned}$$

The multiplication rule with the 3-dimensional representations is

$$3 \otimes 3 = 3_S \oplus 3_A \oplus 1 \oplus 1' \oplus 1''$$

where

$$\begin{aligned} 3_S &= \frac{1}{3} \left(2\alpha_1\beta_1 - \alpha_2\beta_3 - \alpha_3\beta_2, 2\alpha_3\beta_3 - \alpha_1\beta_2 - \alpha_2\beta_1, 2\alpha_2\beta_2 - \alpha_1\beta_3 - \alpha_3\beta_1 \right) \\ 3_A &= \frac{1}{2} \left(\alpha_2\beta_3 - \alpha_3\beta_2, \alpha_1\beta_2 - \alpha_2\beta_1, \alpha_3\beta_1 - \alpha_1\beta_3 \right) \\ 1 &= \alpha_1\beta_1 + \alpha_2\beta_3 + \alpha_3\beta_2 \\ 1' &= \alpha_3\beta_3 + \alpha_1\beta_2 + \alpha_2\beta_1 \\ 1'' &= \alpha_2\beta_2 + \alpha_1\beta_3 + \alpha_3\beta_1 . \end{aligned}$$

Appendix B: Higher order corrections

We consider possible next-to-leading order corrections. Higher-dimensional operators invariant under $SL_2(F_3) \times U(1)_X$ symmetry, suppressed by additional powers of the cutoff scale Λ , could be added to the leading order terms in the superpotential. Then the mass and mixing matrices for fermions can be corrected by both a shift of the vacuum configuration and nontrivial next-to-leading operators contributing to the Yukawa superpotential.

For example, we show that next leading corrections to the renormalizable Majorana neutrino sector can well be under control. In addition to the leading order Yukawa superpotential $W_{\ell\nu}$, we should also consider those higher dimensional operators that could be induced by the flavon fields Φ_T and η which are not charged under the $U(1)_X$. At the next leading order in the Majorana neutrino sector those operators triggered by the field Φ_T are written as $(N^c N^c \Theta \Phi_T)_1 / \Lambda$ and $(N^c N^c \Phi_S \Phi_T)_1 / \Lambda$. Here the first term, after symmetry breaking, is absorbed into the leading order terms in the renormalizable superpotential and the corresponding Yukawa couplings are redefined. On the other hand, the second term could be non-trivial and it can be clearly expressed as

$$\begin{aligned} \Delta W_\nu &= \frac{\hat{y}_1^R}{2\Lambda} (N^c N^c)_1 (\Phi_S \Phi_T)_1 + \frac{\hat{y}_2^R}{2\Lambda} (N^c N^c)_{1'} (\Phi_S \Phi_T)_{1'} + \frac{\hat{y}_3^R}{2\Lambda} (N^c N^c)_{1''} (\Phi_S \Phi_T)_{1''} \\ &+ \frac{\hat{y}_s^R}{2\Lambda} (N^c N^c)_{3_s} (\Phi_S \Phi_T)_{3_s} + \frac{\hat{y}_a^R}{2\Lambda} (N^c N^c)_{3_a} (\Phi_S \Phi_T)_{3_a} . \end{aligned} \quad (\text{B1})$$

Indeed at order $1/\Lambda$, after symmetry breaking, there is a new structure contributing to M_R , whose contribution is written as

$$\Delta M_R = \nabla_T \begin{pmatrix} \tilde{\kappa}_1 + \frac{4}{9}\tilde{\kappa}_s & \tilde{\kappa}_2 + \frac{1}{9}\tilde{\kappa}_s - \frac{1}{6}\tilde{\kappa}_a & \tilde{\kappa}_3 + \frac{1}{9}\tilde{\kappa}_s + \frac{1}{6}\tilde{\kappa}_a \\ \tilde{\kappa}_2 + \frac{1}{9}\tilde{\kappa}_s - \frac{1}{6}\tilde{\kappa}_a & \tilde{\kappa}_3 - \frac{2}{9}\tilde{\kappa}_s - \frac{1}{3}\tilde{\kappa}_a & \tilde{\kappa}_1 - \frac{2}{9}\tilde{\kappa}_s \\ \tilde{\kappa}_3 + \frac{1}{9}\tilde{\kappa}_s + \frac{1}{6}\tilde{\kappa}_a & \tilde{\kappa}_1 - \frac{2}{9}\tilde{\kappa}_s & \tilde{\kappa}_2 - \frac{2}{9}\tilde{\kappa}_s + \frac{1}{3}\tilde{\kappa}_a \end{pmatrix} M, \quad (\text{B2})$$

where

$$\tilde{\kappa}_i \equiv \kappa \hat{y}_i^R / \hat{y}_\Theta \quad (\text{B3})$$

with $i = 1, 2, 3, s, a$. Even though these corrections to the leading order picture seem to non-trivial, these can be kept small, below few percent level due to ∇_T in Eq. (33) by keeping $|\hat{y}_R| \gtrsim |\hat{y}_i^R|$, *i.e.* $\tilde{\kappa} \gtrsim \tilde{\kappa}_i$ with Eq. (67). Then, eventually, after seesawing in Eq. (77) the active neutrino mixing matrix at leading order could not be crucially changed.

Next, considering higher dimensional operators induced by $\Phi_T, \Phi_S, \Theta, \Psi, \eta$ invariant under $SL_2(F_3) \times U(1)_X$ in the driving superpotential W_v , which are suppressed by additional powers of the cut-off scale Λ , they can lead to small deviations from the leading order vacuum configurations. The next leading order superpotential δW_v , which is linear in the driving fields and invariant under $SL_2(F_3) \times U(1)_X \times U(1)_R$, is given by

$$\begin{aligned} \delta W_v = & \frac{1}{\Lambda} \left\{ a_1(\Phi_T \Phi_T)_{\mathbf{3s}}(\Phi_T \Phi_0^T)_{\mathbf{3a}} + a_2(\Phi_T \Phi_T)_{\mathbf{1}}(\Phi_T \Phi_0^T)_{\mathbf{1}} + a_3(\Phi_T \Phi_T)_{\mathbf{1}'}(\Phi_T \Phi_0^T)_{\mathbf{1}''} \right. \\ & + a_4(\Phi_T \Phi_T)_{\mathbf{1}''}(\Phi_T \Phi_0^T)_{\mathbf{1}'} + a_5 \Psi \tilde{\Psi}(\Phi_T \Phi_0^T)_{\mathbf{1}} + a_6(\eta \Phi_T)_{\mathbf{2}}(\eta \Phi_0^T)_{\mathbf{2}} + a_7(\eta \Phi_T)_{\mathbf{2}'}(\eta \Phi_0^T)_{\mathbf{2}''} \left. \right\} \\ & + \frac{1}{\Lambda} \left\{ b_1(\Phi_S \Phi_S)_{\mathbf{3s}}(\Phi_T \Phi_0^S)_{\mathbf{3a}} + b_2(\Phi_S \Phi_S)_{\mathbf{3s}}(\Phi_T \Phi_0^S)_{\mathbf{3s}} + b_3(\Phi_S \Phi_S)_{\mathbf{1}}(\Phi_T \Phi_0^S)_{\mathbf{1}} \right. \\ & + b_4(\Phi_S \Phi_S)_{\mathbf{1}'}(\Phi_T \Phi_0^S)_{\mathbf{1}''} + b_5(\Phi_S \Phi_S)_{\mathbf{1}''}(\Phi_T \Phi_0^S)_{\mathbf{1}'} + b_6 \Phi_0^S(\Phi_S \Phi_T)_{\mathbf{3a}} \Theta \\ & + b_7 \Phi_0^S(\Phi_S \Phi_T)_{\mathbf{3s}} \Theta + b_8 \Phi_0^S(\Phi_S \Phi_T)_{\mathbf{3a}} \tilde{\Theta} + b_9 \Phi_0^S(\Phi_S \Phi_T)_{\mathbf{3s}} \tilde{\Theta} \\ & + b_{10}(\Phi_0^S \Phi_T)_{\mathbf{1}} \Theta \Theta + b_{11}(\Phi_0^S \Phi_T)_{\mathbf{1}} \Theta \tilde{\Theta} + b_{12}(\Phi_0^S \Phi_T)_{\mathbf{1}} \tilde{\Theta} \tilde{\Theta} \left. \right\} \\ & + \frac{\Theta_0}{\Lambda} \left\{ c_1(\Phi_S \Phi_S)_{\mathbf{3s}} \Phi_T + c_2(\Phi_S \Phi_T)_{\mathbf{1}} \tilde{\Theta} \right\} + \frac{\Psi_0}{\Lambda} d_1(\Phi_T \Phi_T)_{\mathbf{3s}} \Phi_T \\ & + \frac{1}{\Lambda} \left\{ f_1(\eta \eta)_{\mathbf{3}}(\eta \eta_0)_{\mathbf{3}} + f_2(\Phi_T \Phi_T)_{\mathbf{3s}}(\eta \eta_0)_{\mathbf{3}} + f_3(\Phi_T \Phi_T)_{\mathbf{1}}(\eta \eta_0)_{\mathbf{1}} + f_4 \Psi \tilde{\Psi}(\eta \eta_0)_{\mathbf{1}} \right\}. \quad (\text{B4}) \end{aligned}$$

By keeping only the first order in the expansion, one can obtain the minimization equations. The corrections to the VEVs, Eqs. (11,13,15), are of relative order $1/\Lambda$ and affect the flavon fields $\Phi_S, \Phi_T, \Theta, \tilde{\Theta}, \eta$ and Ψ , and the vacuum configuration can be modified with relations among the dimensionless parameters $(a_1 \dots a_7, b_1 \dots b_{12}, c_1, c_2, d_1, f_1 \dots f_4)$.

Given the ranges for ∇_Q with $Q = \eta, S, T, \Theta, \Psi$ in Eq. (33), one can expect that the shifts $|\delta\tilde{\Theta}|, |\delta\Theta|/v_\Theta, |\delta v_{S_i}|/v_S, |\delta v_{T_i}|/v_T, |\delta v_{\eta_i}|/v_\eta, |\delta v_\Psi|/v_\Psi$. can be kept small enough, below a few percent level. Then the mixing angles of the active neutrinos in Eq. (77) may not be crucially modified by the next-to-leading order results in FIG. 2 for NO and IO.

Appendix C: The leptonic mixing matrix

In the mass eigenstate basis the PMNS leptonic mixing matrix [26] at low energies is visualized in the charged weak interaction, which is expressed in terms of three mixing angles, $\theta_{12}, \theta_{13}, \theta_{23}$, and three CP -odd phases (one δ_{CP} for the Dirac neutrino and two $\varphi_{1,2}$ for the Majorana neutrino) as

$$U_{\text{PMNS}} = \begin{pmatrix} c_{13}c_{12} & c_{13}s_{12} & s_{13}e^{-i\delta_{CP}} \\ -c_{23}s_{12} - s_{23}c_{12}s_{13}e^{i\delta_{CP}} & c_{23}c_{12} - s_{23}s_{12}s_{13}e^{i\delta_{CP}} & s_{23}c_{13} \\ s_{23}s_{12} - c_{23}c_{12}s_{13}e^{i\delta_{CP}} & -s_{23}c_{12} - c_{23}s_{12}s_{13}e^{i\delta_{CP}} & c_{23}c_{13} \end{pmatrix} P_\nu, \quad (\text{C1})$$

where $s_{ij} \equiv \sin \theta_{ij}$, $c_{ij} \equiv \cos \theta_{ij}$ and P_ν is a diagonal phase matrix what is that particles are Majorana ones.

Appendix D: Axionic domain-wall condition

The quantum numbers associated to charged-leptons are assigned to enforce a positive value of “electromagnetic anomaly $(U(1)_X - [U(1)_{\text{EM}}]^2)/\text{color anomaly } (U(1)_X - [SU(3)_C]^2)$ coefficient” within the range²² $0 < E/N < 4$:

$$\frac{E}{N} = \frac{23}{6}, \quad \text{for } \mathcal{Q}_{y_\tau} = -q, \mathcal{Q}_{y_\mu} = 3q, \mathcal{Q}_{y_e} = -6q; \text{ case-I} \quad (\text{D1})$$

$$\frac{E}{N} = \frac{19}{6}, \quad \text{for } \mathcal{Q}_{y_\tau} = q, \mathcal{Q}_{y_\mu} = 3q, \mathcal{Q}_{y_e} = -6q; \text{ case-II} \quad (\text{D2})$$

$$\frac{E}{N} = \frac{11}{6}, \quad \text{for } \mathcal{Q}_{y_\tau} = -q, \mathcal{Q}_{y_\mu} = -3q, \mathcal{Q}_{y_e} = 6q; \text{ case-III} \quad (\text{D3})$$

where $E = \sum_f (\delta_2^G X_{1f} + \delta_1^G X_{2f})(Q_f^{\text{em}})^2$ and $N = 2\delta_1^G \delta_2^G$. Then, in terms of \mathcal{Q}_y the anomaly-free condition of $U(1)_X \times [\text{gravity}]^2$ is expressed as

$$U(1)_X \times [\text{gravity}]^2 \propto 3 \{4p - \mathcal{Q}_{y_b} + 2(\mathcal{Q}_{Y_s} - \mathcal{Q}_{Y_d} - \mathcal{Q}_{y_c} - \mathcal{Q}_{y_s})\}_{\text{quark}} + \{3p - \mathcal{Q}_{y_1^s} - \mathcal{Q}_{y_2^s} - \mathcal{Q}_{y_3^s} - \mathcal{Q}_{y_e} - \mathcal{Q}_{y_\mu} - \mathcal{Q}_{y_\tau}\}_{\text{lepton}} = 0. \quad (\text{D4})$$

²² This range is derived from the bound ADMX experiment [43] $(g_{a\gamma\gamma}/m_a)^2 \leq 1.44 \times 10^{-19} \text{ GeV}^{-2} \text{ eV}^{-2}$.

This vanishing anomaly, however, does not restrict $\mathcal{Q}_{y_i^\nu}$ (or equivalently $\mathcal{Q}_{y_i^{ss}}$), whose quantum numbers can be constrained by the new neutrino oscillations of astronomical-scale baseline, which will be shown later. With the given above $U(1)_X$ quantum numbers, such $U(1)_X \times [\text{gravity}]^2$ anomaly is free for

$$15 \frac{X_1}{2} = k_2 X_2 \quad \text{with } k_2 = \left\{ \begin{array}{l} \tilde{\mathcal{Q}}_{y_1^s} + \tilde{\mathcal{Q}}_{y_2^s} + \tilde{\mathcal{Q}}_{y_3^s} - 13; \text{ case-I} \\ \tilde{\mathcal{Q}}_{y_1^s} + \tilde{\mathcal{Q}}_{y_2^s} + \tilde{\mathcal{Q}}_{y_3^s} - 11; \text{ case-II} \\ \tilde{\mathcal{Q}}_{y_1^s} + \tilde{\mathcal{Q}}_{y_2^s} + \tilde{\mathcal{Q}}_{y_3^s} - 7; \text{ case-III} \end{array} \right\}. \quad (\text{D5})$$

where $\tilde{\mathcal{Q}}_{y_i^s} = \mathcal{Q}_{y_i^s}/X_2$. We take $k_2 = \pm 15$ for the $U(1)_{X_i}$ charges to be smallest making no axionic domain-wall problem. Hence, for $\tilde{\mathcal{Q}}_{y_1^s} + \tilde{\mathcal{Q}}_{y_2^s} + \tilde{\mathcal{Q}}_{y_3^s} = 28$ (-2) for the case-I; 26 (-4) for the case-II; 22 (-8) for the case-III, the values of k_i are rescaled as

$$k_1 = \pm k_2 = 1, \quad (\text{D6})$$

with $p = k_2$ and $q = k_1$ by $k_1 p = k_2 q = k_1 k_2$. In the present model the color anomaly coefficients are given by $\delta_1^G = 2X_1$ and $\delta_2^G = 3X_2$. Then, the axionic domain-wall condition in Eq. (5) is rewritten as

$$N_1 = 4, \quad N_2 = 3, \quad (\text{D7})$$

ensuring that no axionic domain-wall problem occurs.

Acknowledgments

We thank prof. Hai-Yang Cheng and Xue Xun for useful discussions and kind hospitality, and MH Ahn for useful comments on axion part. This work is supported by the NSFC under Grant No. U1738209.

-
- [1] R. D. Peccei and H. R. Quinn, Phys. Rev. Lett. **38**, 1440 (1977).
 - [2] Y. H. Ahn, Phys. Rev. D **96**, no. 1, 015022 (2017).
 - [3] H. -Y. Cheng, Phys. Rept. **158**, 1 (1988); J. E. Kim, Phys. Rept. **150**, 1 (1987).
 - [4] P. Minkowski, Phys. Lett. B **67**, 421 (1977); T. Yanagida, in Proc. of the Workshop on Unified Theories and Baryon Number in the Universe, ed.O. Sawada and A. Sugamoto, 95 (KEK,

- Japan, 1979); M. Gell-Mann, P. Ramond and R. Slansky, in *Supergravity*, ed. P. Nieuwenhuizen and D. Freeman (North Holland, Amsterdam, 1979); R. N. Mohapatra and G. Senjanovic, Phys. Rev. Lett. **44**, (1980) 912.
- [5] C. D. Froggatt and H. B. Nielsen, Nucl. Phys. B **147**, 277 (1979).
 - [6] Y. H. Ahn, Phys. Rev. D **93**, no. 8, 085026 (2016);
 - [7] F. Feruglio, C. Hagedorn, Y. Lin and L. Merlo, Nucl. Phys. B **775**, 120 (2007).
 - [8] Y. H. Ahn, Phys. Rev. D **91**, 056005 (2015).
 - [9] K. M. Case, R. Karplus and C. N. Yang, Phys. Rev. **101**, 874 (1956); P. H. Frampton and T. W. Kephart, Int. J. Mod. Phys. A **10**, 4689 (1995);
 - [10] A. Aranda, C. D. Carone and R. F. Lebed, Phys. Lett. B **474**, 170 (2000). A. Aranda, C. D. Carone and R. F. Lebed, Phys. Rev. D **62**, 016009 (2000).
 - [11] Y. H. Ahn, Phys. Rev. D **98**, no. 3, 035047 (2018).
 - [12] M. Giannotti, I. G. Irastorza, J. Redondo, A. Ringwald and K. Saikawa, JCAP **1710**, no. 10, 010 (2017).
 - [13] R. Fantechi [NA62 Collaboration], arXiv:1407.8213 [physics.ins-det].
 - [14] F. Wilczek, Phys. Rev. Lett. **49**, 1549 (1982); J. L. Feng, T. Moroi, H. Murayama and E. Schnapka, Phys. Rev. D **57**, 5875 (1998).
 - [15] Y. Ema, K. Hamaguchi, T. Moroi and K. Nakayama, JHEP **1701**, 096 (2017); L. Calibbi, F. Goertz, D. Redigolo, R. Ziegler and J. Zupan, Phys. Rev. D **95**, no. 9, 095009 (2017); Y. Ema, D. Hagihara, K. Hamaguchi, T. Moroi and K. Nakayama, JHEP **1804**, 094 (2018).
 - [16] S. Adler *et al.* [E949 and E787 Collaborations], Phys. Rev. D **77**, 052003 (2008).
 - [17] M. M. Miller Bertolami, B. E. Melendez, L. G. Althaus and J. Isern, JCAP **1410**, no. 10, 069 (2014).
 - [18] M. B. Green and J. H. Schwarz, Phys. Lett. **149B**, 117 (1984).
 - [19] M. Giannotti, I. G. Irastorza, J. Redondo, A. Ringwald and K. Saikawa, JCAP **1710**, no. 10, 010 (2017).
 - [20] J. Isern, E. Garcia-Berro, S. Torres and S. Catalan, Astrophys. J. **682**, L109 (2008);
 - [21] A. Sedrakian, Phys. Rev. D **93**, no. 6, 065044 (2016).
 - [22] R. D. Bolton *et al.*, Phys. Rev. D **38**, 2077 (1988).
 - [23] G. Honecker and W. Staessens, Fortsch. Phys. **62**, 115 (2014); G. Honecker and W. Staessens, J. Phys. Conf. Ser. **631**, no. 1, 012080 (2015). H. Fukuda, M. Ibe, M. Suzuki and

- T. T. Yanagida, Phys. Lett. B **771**, 327 (2017).
- [24] G. Altarelli and F. Feruglio, Nucl. Phys. B **720**, 64 (2005); Nucl. Phys. B **741**, 215 (2006); Rev. Mod. Phys. **82**, 2701 (2010).
- [25] L. Wolfenstein, Phys. Rev. Lett. **51**, 1945 (1983).
- [26] C. Patrignani et al. (Particle Data Group), Chin. Phys. C, 40, 100001 (2016).
- [27] L. L. Chau and W. Y. Keung, Phys. Rev. Lett. **53**, 1802 (1984).
- [28] <http://ckmfitter.in2p3.fr>.
- [29] S. Antusch, J. Kersten, M. Lindner, M. Ratz and M. A. Schmidt, JHEP **0503**, 024 (2005).
- [30] L. B. Leinson, Phys. Lett. B **741**, 87 (2015).
- [31] L. B. Leinson, JCAP **1408**, 031 (2014).
- [32] J. Isern, E. Garcia-Berro, S. Torres and S. Catalan, Astrophys. J. **682**, L109 (2008); J. Isern, S. Catalan, E. Garcia-Berro and S. Torres, J. Phys. Conf. Ser. **172**, 012005 (2009); J. Isern, M. Hernanz and E. Garcia-Berro, Astrophys. J. **392**, L23 (1992).
- [33] A. V. Artamonov *et al.* [E949 Collaboration], Phys. Rev. Lett. **101**, 191802 (2008).
- [34] Y. Ema, D. Hagihara, K. Hamaguchi, T. Moroi and K. Nakayama, arXiv:1802.07739 [hep-ph]; F. Bjrkeroth, E. J. Chun and S. F. King, Phys. Lett. B **777**, 428 (2018); F. Arias-Aragon and L. Merlo, JHEP **1710**, 168 (2017); J. C. Gmez-Izquierdo, Eur. Phys. J. C **77**, no. 8, 551 (2017); Y. Ema, K. Hamaguchi, T. Moroi and K. Nakayama, JHEP **1701**, 096 (2017); L. Calibbi, F. Goertz, D. Redigolo, R. Ziegler and J. Zupan, Phys. Rev. D **95**, no. 9, 095009 (2017); T. Nomura, Y. Shimizu and T. Yamada, JHEP **1606**, 125 (2016);
- [35] I. Esteban, M. C. Gonzalez-Garcia, M. Maltoni, I. Martinez-Soler and T. Schwetz, JHEP **1701**, 087 (2017).
- [36] G. G. Raffelt, J. Redondo and N. V. Maira, Phys. Rev. D **84**, 103008 (2011).
- [37] H. Umeda, N. Iwamoto, S. Tsuruta, L. Qin and K. Nomoto, astro-ph/9806337; J. Keller and A. Sedrakian, Nucl. Phys. A **897**, 62 (2013).
- [38] J. Redondo, JCAP **1312**, 008 (2013);
- [39] N. Viaux, M. Catelan, P. B. Stetson, G. G. Raffelt, J. Redondo, A. A. R. Valcarce and A. Weiss, Phys. Rev. Lett. **111**, 231301 (2013).
- [40] G. G. Raffelt, Phys. Lett. B **166**, 402 (1986); S. I. Blinnikov and N. V. Dunina-Barkovskaya, Mon. Not. Roy. Astron. Soc. **266**, 289 (1994).
- [41] E. Aprile *et al.* [XENON100 Collaboration], Phys. Rev. D **90**, no. 6, 062009 (2014);

- [42] C. Fu *et al.* [PandaX Collaboration], Phys. Rev. Lett. **119**, no. 18, 181806 (2017).
- [43] S. J. Asztalos, R. F. Bradley, L. Duffy, C. Hagmann, D. Kinion, D. M. Moltz, L. J. Rosenberg and P. Sikivie *et al.*, Phys. Rev. D **69**, 011101 (2004).
- [44] Y. H. Ahn and E. J. Chun, Phys. Lett. B **752**, 333 (2016).
- [45] A. de Gouvea, W. C. Huang and J. Jenkins, Phys. Rev. D **80**, 073007 (2009).
- [46] L. A. Anchordoqui, H. Goldberg, F. Halzen and T. J. Weiler, Phys. Lett. B **621**, 18 (2005).
- [47] P. F. Harrison, D. H. Perkins and W. G. Scott, Phys. Lett. B **530**, 167 (2002).
- [48] <http://t2k-experiment.org>.
- [49] <https://www-nova.fnal.gov>; P. Adamson *et al.* [NOvA Collaboration], Phys. Rev. Lett. **118**, no. 15, 151802 (2017).
- [50] <https://www-numi.fnal.gov>.
- [51] K. Abe *et al.* [T2K Collaboration], Phys. Rev. Lett. **112**, no. 18, 181801 (2014); P. Adamson *et al.* [NOvA Collaboration], Phys. Rev. Lett. **116**, no. 15, 151806 (2016); K. Abe *et al.* [T2K Collaboration], arXiv:1701.00432 [hep-ex].
- [52] <http://icecube.wisc.edu>.
- [53] S. Gariazzo, M. Archidiacono, P. F. de Salas, O. Mena, C. A. Ternes and M. Trtola, arXiv:1801.04946 [hep-ph].
- [54] M. C. Gonzalez-Garcia, M. Maltoni, J. Salvado and T. Schwetz, JHEP **1212**, 123 (2012); M. C. Gonzalez-Garcia, M. Maltoni and T. Schwetz, Nucl. Phys. B **908**, 199 (2016) [arXiv:1512.06856 [hep-ph]].
- [55] A. Gando *et al.* [KamLAND-Zen Collaboration], Phys. Rev. Lett. **110**, no. 6, 062502 (2013); M. Auger *et al.* [EXO Collaboration], Phys. Rev. Lett. **109**, 032505 (2012); M. Agostini *et al.* [GERDA Collaboration], arXiv:1307.4720 [nucl-ex]; H. V. Klapdor-Kleingrothaus, A. Dietz, L. Baudis, G. Heusser, I. V. Krivosheina, S. Kolb, B. Majorovits and H. Pas *et al.*, Eur. Phys. J. A **12**, 147 (2001); C. E. Aalseth, F. T. Avignone, R. L. Brodzinski, S. Cebrian, E. Garcia, D. Gonzales, W. K. Hensley and I. G. Irastorza *et al.*, Phys. Rev. D **70**, 078302 (2004).
- [56] K. Abe *et al.* [T2K Collaboration], Phys. Rev. D **96**, no. 9, 092006 (2017).